Understanding Changes in Terrestrial Water Storage over West Africa between 2002 and 2014

Christopher Ndehedehe[a,c], Joseph Awange[a,b,e], Nathan Agutu[a,d], Michael Kuhn[a], and Bernhard Heck[b]

[a] *Western Australian Centre for Geodesy and The Institute for Geoscience Research Curtin University, Perth, Australia.*
[b] *Geodetic Institute, Karlsruhe Institute of Technology, Karlsruhe, Germany.*
[c] *Department of Geoinformatics and Surveying, University of Uyo, Nigeria.*
[d] *Department of Geomatic Engineering and Geospatial Information systems JKUAT, Nairobi, Kenya.*
[e] *Department of Geophysics, Kyoto University, Japan*

Abstract

With the vast water resources of West Africa coming under threat due to the impacts of climate variability and human influence, the need to understand its terrestrial water storage (TWS) changes becomes very important. Due to the lack of consistent in-situ hydrological data to assist in the monitoring of changes in TWS, this study takes advantage of the Gravity Recovery and Climate Experiment (GRACE) monthly gravity fields to provide estimates of vertically integrated changes in TWS over the period 2002-2014, in addition to satellite altimetry data for the period 1993-2014. In order to understand TWS variability over West Africa, Principal Component Analysis (PCA), a second order statistical technique, and Multiple Linear Regression Analysis (MLRA) are employed. Results show that dominant patterns of GRACE-derived TWS changes are observed mostly in the West Sahel, Guinea Coast, and Middle Belt regions of West Africa. This is probably caused by high precipitation rates at seasonal and inter-annual time scales induced by ocean circulations, altitude and physiographic features. While the linear trend for the spatially averaged GRACE-derived TWS changes over West Africa for the study period shows an increase of 6.85 ± 1.67 mm/yr, the PCA result indicates a significant increase of 20.2 ± 5.78 mm/yr in Guinea, a region with large inter-annual variability in seasonal rainfall, heavy river discharge, and huge groundwater potentials. The increase in GRACE-derived TWS during this period in Guinea, though inconsistent with the lack of a significant positive linear trend in TRMM based precipitation, is attributed to a large water surplus from prolonged wet seasons and lower evapotranspiration rates, leading to an increase in storage and inundated areas over the Guinea region. This increase in storage, which is also the aftermath of cumulative increase in the volume of water not involved in

surface runoff, forms the huge freshwater availability in this region. However, the relatively low maximum water levels of Kainji reservoir in recent times (i.e., 2004/2005, 2007/2008, and 2011/2012) as observed in the satellite altimetry-derived water levels might predispose the Kainji dam to changes that probably may have a negative impact on the socio-economic potentials of the region. GRACE-derived TWS is not well correlated with TRMM-based precipitation in some countries of West Africa and apparently indicates a lag of two months over much of the region. On the other hand, the regression fit between GLDAS-derived TWS and GRACE-derived TWS shows R^2 of 0.85, indicating that trends and variability have been well modelled.

Keywords: GRACE, PCA, TRMM, GLDAS, Satellite Altimetry, Multiple Linear Regression Analysis

1. Introduction

With an estimated population of 300 million people whose livelihood depends on rain-fed agriculture (see, e.g., USAID, 2013; Roudier et al., 2011; Amani et al., 2007), West Africa is one of the regions in the world with highly variable and extreme climatic conditions (i.e., droughts and floods), which impacts directly on the hydrological cycle and the human population. Despite its vast water resources, which includes lakes, rivers, wetlands, and groundwater systems, West Africa has a history of vulnerability to the impacts of climate change, which threatens these water resources and agriculture (e.g., Coe and Foley, 2001; Roudier et al., 2011; Okpara et al., 2013; Oyebande and Odunuga, 2010; Ojo et al., 2004).

More often than not, the region is subjected to food insecurity, famine, health issues, and social instability due to water related problems induced by the frequency and persistence of extreme hydrological/hydro-climatological conditions (e.g., droughts and floods) (see, e.g., Okpara et al., 2013; Descroix et al., 2009; Boone et al., 2009; Vierich and Stoop, 1990). Therefore, understanding the spatio-temporal variability of changes in terrestrial water storage (TWS) (i.e., the total of surface waters, soil moisture, canopy storage, and groundwater) in this region can support sustainable decisions and effective management of water resources. In addition, it can also provide information on the hydrological footprints, which probably can help reveal the impacts of climate variability on the region's TWS.

Furthermore, in West Africa, changes in any component of the TWS do have socio-economic and environmental implications (e.g., Grippa et al., 2011). For example, as described in Moore

and Williams (2014) in a recent study in Africa, the surface waters are needed to maintain fisheries, which are a principal contributor to the food basket of the region. Consequently, changes to any component of these surface waters (i.e., lakes and rivers) or groundwater resources might jeopardise the livelihood and the economic viability of the region. Apparently, for a region such as West Africa that depends heavily on rain-fed agriculture; reduced rainfall and freshwater availability may lead to crop failure, and low agricultural productivity (Xie et al., 2012; Vierich and Stoop, 1990). This ultimately will affect agricultural development and the economy of the region. Besides the reduced freshwater availability occasioned by changes in rainfall patterns of the region (Forootan et al., 2014), the increasing irrigation development (Xie et al., 2012), ecosystem functioning and other various forms of anthropogenic influence puts water resources at risk (e.g., Coe and Foley, 2001), hence the need to examine the changes in TWS and its variability over West Africa, which in the long term can support effective allocation, governance, and management.

Changes in TWS, be they groundwater, soil moisture, canopy storage, surface waters (i.e., lakes, wetlands, and rivers) remain one of the most critical components of the hydrological cycle. However, estimating these changes in TWS over West Africa remains a major challenge due to few in-situ monitoring stations, lack of large scale hydrological data, and unreliable field measurements amongst others. While Grippa et al. (2011) specifically noted that the monitoring of water budget components in West Africa are hampered by scarcity of in-situ measurements, Anayah and Kaluarachchi (2009) reported that the monitoring of groundwater in the upper east region of northern Ghana started in 2005 and continued until the end of 2008 (i.e., from 5 monitoring wells). Local measurements from dedicated networks such as the AMMA-CATCH[1] hydro-meteorological observing system have been used in validation studies (e.g., Gosset et al., 2013) and to characterize rainfall regime for the Gourma region located in Mali (e.g., Frappart et al., 2009). However, hydrological studies over large spatially heterogenous areas remain difficult as the AMMA-CATCH networks are highly insufficient and only available in few countries (i.e., Niger, Mali, and Benin). Besides the scarcity and the incomplete records of in-situ data in the sub-regions due to limited and degraded weather hydrological infrastructures precipitated by poor government funding, Nicholson et al. (2000)

[1]African Monsoon Multidisciplinary Analysis-Couplage Atmosphere Tropicale Cycle Hydrologique (Lebel et al., 2009)

reported that the acquisition of rainfall data despite its availability was largely hindered by political and economic instability, in addition to government policies. Due to these sparse in-situ meteorological and hydrological monitoring networks in West Africa, degraded hydrological infrastructures, data inaccessibility, and the gaps in routine measurements of relevant hydrological variables (e.g., river discharge, groundwater), our understanding of the spatio-temporal patterns of TWS changes is limited, hence the need for a large scale holistic assessment of water storage estimation.

Due to the lack of in-situ hydrological data to assist in the accurate monitoring of TWS changes, indices such as effective drought index (EDI), standard precipitation index (SPI), and palmer drought severity index (PDSI) have been used as proxies for monitoring water availability and hydrological conditions (see, e.g., Laux, 2009; Heim, 2002; McKee et al., 1993, 1995). However, these indices do not account for the changes in the state of other water storage components (e.g., groundwater) (Long et al., 2013), which is an important resource for livelihood. While it has been reported that these indices are associated with uncertainties (see, e.g., Ahmed et al., 2014), the use of hydrological models has shown relatively good performance (Pedinotti et al., 2012) on the one hand, and inconsistent results on the other hand (Xie et al., 2012). However, land water storage output from models underestimate changes in water storage, and might be restricted due to limited data for evaluation and calibration purposes (Boone et al., 2009; Schuol and Abbaspour, 2006). In order to circumvent this problem, previous studies have combined remote sensing data and outputs from models to improve the estimation of changes in TWS (e.g., Wagner et al., 2009; Leblanc et al., 2007).

Since March 2002, the Gravity Recovery and Climate Experiment (GRACE) satellite mission under the auspices of National Aeronautic and Space Administration (NASA) in the United States and its German counterpart the Deutsches Zentrum für Luft-und Raumfahrt (DLR) has been collecting and archiving time variable monthly gravity fields (Tapley et al., 2004). These monthly gravity fields are provided as sets of spherical harmonic coefficients, which can be inverted to global and regional estimates of vertically integrated TWS at a spatial resolution of few hundred kilometres or more (Swenson and Wahr, 2007, 2002; Wahr et al., 1998).

GRACE data has been used in the estimation of changes in TWS over West Africa in recent times. For instance, Grippa et al. (2011) in a validation study, compared estimated TWS variations from different GRACE products with outputs from 9 land surface models operating

within the framework of the African Monsoon Multidisciplinary Analysis Land Surface Intercomparison Project (ALMIP). From the study, model outputs had a good agreement with GRACE-derived TWS changes. However, the analysis did not include the Western Sahel and some parts of Guinea coast, the region whose general rainfall pattern is highly influenced by ocean circulations and physiographic features. Ferreira et al. (2012, 2014) estimated mass changes and sink terms over the Volta basin in West Africa while Forootan et al. (2014) proposed a prediction approach of TWS over West Africa for a duration of two years using a combination of past GRACE data, precipitation, and SST over the oceans. Still in West Africa, while Nahmani et al. (2012) in a comparative study showed how the observed vertical deformation component from GPS data was fairly consistent with regional-scale estimates from GRACE satellite products and geophysical models, Hinderer et al. (2009), had previously compared in-situ data from GPS with satellite observations such as GRACE in a project labelled Gravity and Hydrology in Africa. Furthermore, at continental and basin-wide scales, GRACE data have been used to investigate trends, and seasonal cycles of the various TWS components (see, e.g., Ahmed et al., 2014; Awange et al., 2013, 2014a,b; Ramillien et al., 2014). For example, results of GRACE TWS solutions computed over Africa from 2003 to 2012 in Ramillien et al. (2014) indicate a water loss from the North Saharan aquifers.

In order to improve our understanding of the land water storage over West Africa and to further extend the studies mentioned above, this study attempts to highlight the recent annual and seasonal variability of TWS changes for the period 2002-2014. Contrary to previous studies in the region, the approach here is to analyse the variability and the relationship between GRACE-derived TWS changes and rainfall patterns over West Africa using principal component analysis (PCA) (Jolliffe, 2002; Preisendorfer, 1988) and multiple linear regression analysis (MLRA). The study looks into the inter-annual and seasonal variability of TWS changes, lake height variations of water reservoirs, and precipitation patterns. To evaluate GRACE-derived TWS changes over West Africa, total water storage content (TWSC) from the Global Land Data Assimilation System (GLDAS) (Rodell et al., 2004) were also explored.

Therefore, this study explores hydrological fluxes such as precipitation and satellite altimetry data, alongside with TWS changes from GRACE and GLDAS in order to understand the spatio-temporal dynamics of these hydrological variables and the available water resources that can support sustainable agriculture and ecosystem functioning. Specifically the study seeks to (i) identify trends and dominant patterns of TWS changes and its relation to precipitation

over West Africa and (ii) understand the annual seasonal cycles of TWS and precipitation changes over West Africa and the response time between them.

The remainder of the study is segmented as follows; in section 2, a brief introduction to the study area is provided while in section 3, a discussion on the data and methodology is given. This is followed by analysis and discussion of the results in section 4. The conclusion of the study is provided in section 5.

2. West Africa

2.1. Location

West Africa is located between latitudes 0°N to 20°N and longitudes 20°W to 20°E (Fig. 1) and comprises a group of 16 countries covering an area of approximately 7.5 Million km^2. The two major geographical zones are the countries of the gulf of Guinea (i.e., the area between latitudes 4°N and 8°N), and the Sahelian countries (e.g., Amani et al., 2007). The southern boundary is the Atlantic ocean; on the north is the Sahara desert, while the eastern boundary is flanked by the Cameroon mountains.

2.2. Climate

The climate of West Africa is governed by the seasonal migration of the intertropical convergence zone (ITCZ) (e.g., McSweeney et al., 2010). The location, position, and intensity (strength) of both the circulation features and ITCZ are responsible for the extreme wet and dry conditions, and intra-annual rainfall distribution in the Sahel and likewise the gulf of Guinea (Nicholson and Webster, 2007; Lebel and Ali, 2009; Nicholson, 2013; Nicholson and Grist, 2001). While rainfall ranges from less than 200 mm/yr in the Sahelian countries to over 2000 mm/yr in the gulf of Guinea, an increasing annual trend in temperature of 0.20°C/yr has been observed (e.g., Okpara et al., 2013; Ojo et al., 2004). Rain seasons in the gulf of Guinea occur between April-June and July-September, with the wettest months being June and September or sometimes October (Nicholson et al., 2000). In the Sahel and fringe of the desert, the rain season takes place between June and September with maximum rainfall occurring in August. SSSS

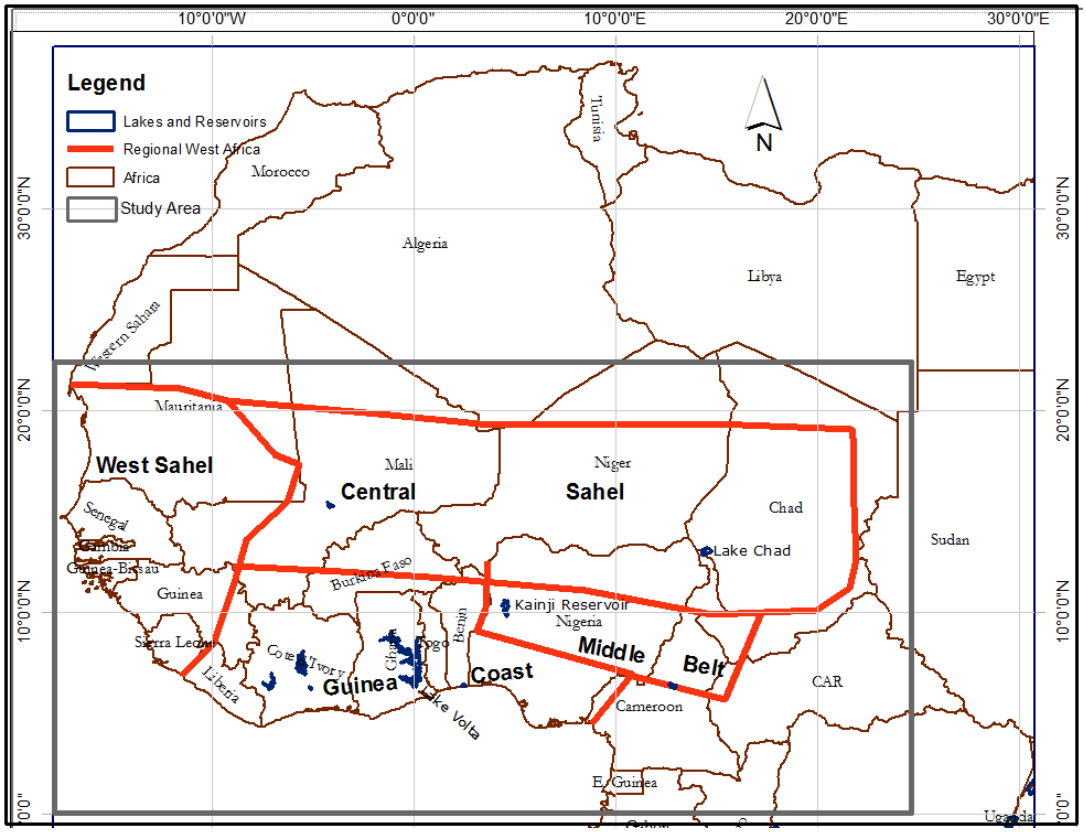

Figure 1: Study area showing the definitions of sub-regions of West Sahel (WS), Central Sahel (CS), Guinea Coast (GC), and Middle Belt modified after Diatta and Fink (2014). .

3. Data and Methodology

3.1. Data

3.1.1. Gravity Recovery and Climate Experiment (GRACE)

The GRACE satellite mission has been in space since March 2002, collecting monthly gravity fields used to estimate global changes in TWS (Tapley et al., 2004). GRACE time-variable gravity field products have been frequently used to study the Earth's water storage changes at basin, continental, and global scales (Ferreira et al., 2012; Grippa et al., 2011; Ramillien et al., 2008). The standard GRACE products, which are usually referred to as sets of spherical harmonic coefficients, were used in estimating TWS changes. These spherical harmonic coefficients do suffer from signal attenuation and satellite measurement errors causing noise in the higher degree coefficients (Landerer and Swenson, 2012; Swenson and Wahr, 2002). Consequently, GRACE data undergo filtering in the form of spatial averaging and smoothing in order to reduce the effect of noise (see, e.g., Wouters et al., 2014; Swenson and Wahr, 2007). Prior to the smoothing of GRACE data, degree 2 coefficients were replaced with estimates from

satellite laser ranging (Cheng et al., 2013) while the degree 1 coefficients provided by Swenson et al. (2008) were used. This is a conventional practice since GRACE does not provide changes in degree 1 coefficients (i.e., C_{10}, C_{11}, and S_{11}), and is also affected by large tide-like aliases in the degree 2 coefficients (i.e., C_{20}). The GRACE Release-05 (RL05) spherical harmonic coefficients truncated at degree and order 60 from Center for Space Research (CSR), covering the period 2002-2014 is used in this study to compute changes in TWS. The three well known processing centers such as the CSR, GeoForschungsZentrum (GFZ) and the Jet Propulsion Laboratory (JPL) use different algorithms to compute gravity field harmonic coefficients from the raw GRACE observations. Over West Africa, Grippa et al. (2011) observed that seasonal water storage computed from the three GRACE products show significant differences, as opposed to their temporal evolutions, which were rather consistent. We use the CSR data set because of its wide application in continent-wide studies.

The fully normalised spherical harmonic coefficients were smoothed using the DDK2 decorrelation filter (Kusche et al., 2009) before converting it to equivalent water heights (EWH) following the approach of Wahr et al. (1998). While taking notice of Landerer and Swenson (2012) computed TWS solution, which uses an isotropic Gaussian averaging filter, the choice of the DDK2 filter used here is because it embodies both decorrelation and smoothing and also accommodates better the an-isotropic GRACE error structure (Kusche, 2007). The computed TWS was synthesised on a 1° x 1° grid and then rescaled in order to restore the geophysical signal loss caused by the effect of spatial averaging using the de-correlation filter during the post-processing of the GRACE data (Long et al., 2015; Landerer and Swenson, 2012). Considering the progress made so far and the advances in the use of GRACE data, i.e., from validation to full utilization especially in hydrological studies, rescaling GRACE data in order to remedy signal loss caused by the filtering is critical. For instance, Landerer and Swenson (2012), emphasized that if the effect of the filter is not accounted for in the transformed GRACE observations, the signal attenuation will become an error in the residual in the regional water balance or will serve as a constraint in water budget closure. In appendix A, we show the impact of filtering on CSR and JPL GRACE products and their relationship with model-generated water storage. In particular, the effect of the DDK2 filter on computed GRACE-derived TWS before and after restoring the geophysical signal loss was measured by comparing it with the GLDAS-TWS. The rescaled monthly TWS grids had a few random gaps of up to 12 months in between that were filled through interpolation, which is a common

reconstruction method for hydrological time series (e.g., Santos et al., 2010). This is particularly important for principal component analysis, which requires continuous spatio-temporal data (Rangelova et al., 2007). Though we have also computed GRACE derived TWS using coefficients from those of JPL, however, the desired objectives of this study are realized by using a single product, given the observed consistency in the temporal patterns of CSR and JPL (see Appendix A). Also, Ferreira et al. (2012) showed similar consistency between the time series of GRACE-derived TWS changes using GFZ and CSR coefficients in the region.

3.1.2. Tropical Rainfall Measuring Mission (TRMM)

The TRMM 3B43 (Huffman et al., 2007; Kummerow et al., 2000) provides monthly precipitation estimates of high temporal (month) and spatial (0.25° x 0.25°) resolution, with global coverage between the geographic latitudes 50°S and 50°N. For this study, monthly TRMMv7 3B43 precipitation rates from National Aerospace and Space Administration (NASA) Goddard Space Flight Center (GSFC) covering the period 1998-2013 was used to analyse the spatio-temporal variability of rainfall over West Africa. TRMM data has been validated (i.e., comparing satellite rainfall observations with gauge datasets) for the region (e.g., Nicholson et al., 2003) and significantly improved (e.g., Duan and Bastiaanssen, 2013). Also, especially for West Africa, TRMM validation using in-situ data showed zero bias (i.e., the magnitude of TRMM was consistent with those of gauges), with a root mean square error (RMSE) of 0.7/0.9 mm/day for the seasonal and August rainfall (e.g., Nicholson, 2013). Unlike East Africa where the Global Precipitation Climatology Center (GPCC) gauge dataset is inconsistent with TRMM, over West Africa, the GPCC gauge data shows good agreement with TRMM (see, Paeth et al., 2012; Nicholson et al., 2003). Further, the monthly TRMM precipitation were resampled into 1° x 1° in order to maintain a common spatial resolution with other datasets such as GRACE-TWS solutions.

3.1.3. Global Land Data Assimilation System (GLDAS)

GLDAS (Rodell et al., 2004) drives four land surface models (Mosaic, Community Land Model (CLM), Variable Infiltration Capacity (VIC), and Noah) to produce different fields of the land surface (e.g., Hassan and Jin, 2014). In this study, GLDAS-derived monthly total water storage content (TWSC) at 1° x 1° spatial resolution was used for a comparative analysis to evaluate GRACE data over the region. In addition, similar to Landerer and Swenson (2012) and Long et al. (2015), the derived TWSC from GLDAS was also used to rescale the GRACE-

derived TWS in order to restore the signal loss due to filtering. Also, we highlight briefly that the relationship between the original and DDK2-filtered GLDAS data was used to obtain the scale factor. The data covering the years 2002-2013 was obtained from the Goddard Earth Sciences Data and Information Services Center (GESDICS)[2].

3.1.4. Satellite Altimetry

Lake height variations computed from TOPEX/POSEIDON (T/P), Jason-1 and Jason-2/OSTM altimetry provided by the United States Department of Agriculture (USDA) was used in the study as auxiliary information to analyse water reservoirs in the study area. Time series of lake levels can be downloaded from www.pecad.fas.usda.gov/cropexplorer/globalreservoir and the hydroweb Laboratoire dEtude en Geophysique et Oceanographie Spatiale (LEGOS) database. The data covering the period 1993 to 2013 was used in the study to analyse lake height variation. We rely on altimetry data for this study since the estimated errors of lake height variation with respect to the reference mean level for Lake Volta, Lake Chad, and Kainji dam are mostly in the sub-centimeter range. The USDA lake height variation time series used in this study were already smoothed with a median type filter to eliminate outliers and reduce high frequency noise.

3.2. Methodology

3.2.1. Principal Component Analysis (PCA)

Principal component analysis (PCA) is an extraction technique that is used to reduce the dimension of large multivariate data, and at the same time account for the most dominant variations in the original data set (e.g., Jolliffe, 2002; Martinez and Martinez, 2005; Westra et al., 2010; Preisendorfer, 1988). Its mathematical simplicity and the ability to explain the optimised variance, using a small number of principal components, has probably made this method the most widely used statistical data analysis tool in climate science (Westra et al., 2010). In addition to its simplicity, the choice of PCA in this study is also due to its capability to isolate both inter-annual signals, and long-term periodic variations (e.g., Rangelova et al., 2007). Fundamentally, PCA reduces the dimensions of multivariate data by creating new variables that are linear functions of the original variables. Given k variables at a given time period i, the linear combinations for k principal components (PCs) are

[2]http://grace.jpl.nasa.gov/data/gldas/

$$\begin{bmatrix} y_{i,1} = p_{11}\mathbf{x}_{i,1} + p_{12}\mathbf{x}_{i,2} + p_{13}\mathbf{x}_{i,3} \ + ... \ + \ p_{1k}\mathbf{x}_{i,k} \\ y_{i,2} = p_{21}\mathbf{x}_{i,1} + p_{22}\mathbf{x}_{i,2} + p_{23}\mathbf{x}_{i,3} \ + ... \ + \ p_{2k}\mathbf{x}_{i,k} \\ ... \\ ... \\ y_{i,k} = p_{k1}\mathbf{x}_{i,1} + p_{k2}\mathbf{x}_{i,2} + p_{k3}\mathbf{x}_{i,3} \ + ... \ + \ p_{kk}\mathbf{x}_{i,k} \end{bmatrix} \qquad i = 1, ..., n \qquad (1)$$

The data matrix $\mathbf{x}_{i,k}$ contains rows representing the time i in months and k, the variables, i.e., the observations, which in our case is TWS or rainfall. In the linear combinations above (Eq. 1) the y values are orthogonal and also the new uncorrelated variables called the PCs such that y_{i1} explains the highest variability while y_{i2} up to y_{ik} explain the remaining variance. The coefficients of the linear combinations are called loadings (i.e., the eigenvectors) and they provide the weights of the original variables in the PCs. The eigenvalues (i.e., the amount of covariance in time explained by each eigenvector) and eigenvectors, which is also referred to as empirical orthogonal functions (EOFs) can be derived from the sample covariance matrix or correlation matrix of the centered data matrix $\mathbf{x}_{i,k}$. The EOF is the spatial distribution or the spatial patterns of rainfall or TWS while the EOF/PC pair is called the PCA mode. In our case, the covariance PCA method was used since it is more ideal for climate analysis, in addition to extracting PCs that emphasize areas with very high temporal variability (e.g., Nicholson, 2014; Jolliffe, 2002). While the eigenvectors (e.g., p_{11}, p_{12}, p_{13}... p_{kk}), which have been normalised are the loadings, each eigenvalue (i.e., $\lambda_1 \geq \lambda_2 \geq \lambda_3 ... \lambda_k$) explains the fraction of the total variance explained by the loadings (e.g., Santos et al., 2010). Further details on the choice of dimensions to reduce (i.e., dominant modes), geometric and statistical properties of PCA can be found e.g., in Jolliffe (2002). The use of a component extraction method such as PCA to decompose GRACE data, and satellite precipitation data into sets of principal components (PCs) and EOFs might probably help address some questions such as what are the trends and dominant spatio-temporal patterns of TWS variations in the region. Most importantly, using PCA in this study will provide a good knowledge of the spatio-temporal distribution of TWS and rainfall, which is important for water resources planning and understanding the impacts of climate on the hydrological system of West Africa. Hence, PCA was used in this study to analyse spatio-temporal patterns of changes in TWS and precipitation over West Africa.

3.2.2. Multiple Linear Regression Analysis(MLRA)

The MLRA method is a statistical technique used to model the relationships between a dependent variable and one or more independent variables. It uses a least squares approach and has been widely applied in hydrology and climate science to explain the possible relationships between key variables (see, e.g., Diatta and Fink, 2014; Seidou et al., 2007). In order to understand the seasonal and inter-annual variations in the data series (i.e., TWS and rainfall) at a given grid point, the regression model of the form (e.g., Rieser et al., 2010):

$$X(t) = \beta_0 + \beta_1 t + \beta_2 sin(2\pi t) + \beta_3 cos(2\pi t) + \beta_4 sin(4\pi t) + \beta_5 cos(4\pi t) + \varepsilon, \tag{2}$$

has been fitted to the time series of the data. X(t) is TWS or rainfall at time t, β_0 is a constant offset, β_1 is the linear trend, β_2 and β_3 account for the annual signal while β_4 and β_5 represent the semi-annual signals. The model bias ε is taken as the deviation between model outputs and observations. Least squares fitting approach is used to estimate the regression coefficients, and the selected harmonic components (i.e., annual amplitude and semi-annual amplitude) are computed as:

$$Annual\ Amplitude = \sqrt{(\beta_2)^2 + (\beta_3)^2}, \tag{3}$$

$$Semi\ Annual\ Amplitude = \sqrt{(\beta_4)^2 + (\beta_5)^2}, \tag{4}$$

and the root-mean-square-error was computed as:

$$RMSE = \sqrt{\frac{1}{n}\sum_{i=1}(x_{obs} - x_{sim})^2}, \tag{5}$$

where x_{obs} and x_{sim} are observations and simulated values from the regression model respectively for n months. In order to assess the model's fitness in simulating TWS and rainfall, the coefficient of multiple determinations was computed for each grid point of the data. Besides the root mean square errors (RMSEs) and the coefficients of multiple determinations, the bias (i.e., difference between the true value being estimated and the expected value of an estimator) was also computed to further evaluate the performance of the MLRA over West Africa. Further, the use of MLRA will provide insight regarding the extent to which simulations of TWS and precipitation can be relied upon. This method was applied here to model the trend, annual and semi-annual components of TWS changes and precipitation over West Africa.

3.2.3. Variability Index and Trends

To examine the variation in trends, and further analyse the seasonal variations in the region for the period investigated, the variability index was computed for precipitation and TWS, from which annual and semi-annual components have been removed using MLRA. In essence, this study analysed the monthly variability of trends and seasonal signals for the two products. The reason for this approach is to help classify the time series of changes in TWS and rainfall residuals, which consists of trends and seasonal components, into different climatic regimes such as wet, dry, normal, and extreme (L´Hôte et al., 2002). For precipitation, the variability index is computed as standardised precipitation departure while for TWS, it is computed as standardised TWS deviation:

$$\delta_{TWS/P} = (X_{TWS/P} - \mu)/\sigma, \tag{6}$$

where $\delta_{TWS/P}$ is the variability index for the TWS or rainfall (P), $X_{TWS/P}$ is the data (i.e., TWS or P) averaged over the region (i.e., over land), μ and σ are the mean and standard deviation for the data over the study period respectively, e.g., using all spatio-temporal data. Besides the computation of standardised deviation for TWS and precipitation, a trend was fitted into the monthly grids of rainfall for the period 2002-2013. In addition to this, rainfall was averaged over the region in order to understand the evolving annual amplitude of rainfall from the temporal patterns. In order to decrease the strong effect of the annual signal in the spatially averaged rainfall over the region, the monthly rainfall was smoothed using a moving average filter. Also, the least squares method was used to estimate the trends in (i) the time series of averaged TWS for the period between 2002-2014 and (ii) the temporal evolution of relevant PC modes derived from TWS decomposition using the PCA method.

3.2.4. Correlation Analysis

Several approaches appropriated for modelling the relationships between multivariate data measured at different times include autocorrelation, coherence analysis, dynamic factor analysis, cross-correlation, etc., (Boker et al., 2002). In this study, Pearsons correlation coefficient is used to examine the strength of agreement between two different hydrological variables (e.g., rainfall and TWS) while cross-correlation is used to determine the time lag between the hydrological signals (i.e., TRMM based precipitation and GRACE-derived TWS). Monthly grids of precipitation and GLDAS TWSC were correlated with that of GRACE-derived TWS at 95% confidence level in order to study the relations between them. In the cross-correlation

approach, the position of the peak value indicates the time offset when the peak association occurred (i.e., when the two signals are the most similar) in the hydrological time series. In order to understand the response time (i.e., the time lag with maximum correlation) of TWS to rainfall in the region, the cross-correlation method was used. Besides the cross correlation approach, the seasonal cycles of rainfall and TWS were also used to understand the lag relationship. A regression fit was also applied to understand the relationship and the variability between time series of GRACE-derived TWS and GLDAS TWSC for the common period (i.e., 2002-2014).

4. Results and Discussions

4.1. Dominant Patterns of Total Water Storage (TWS) over West Africa

The PCA method has been used to identify the dominant spatio-temporal patterns of changes in TWS over West Africa within the period of 2002 to 2014. For statistical inference, the TWS grid is decomposed into sets of principal components (PCs, i.e., the temporal patterns), and their corresponding empirical orthogonal functions (EOFs, i.e., the spatial patterns) using the PCA covariance method. While the EOFs (also referred to as the eigenvectors) are standardised using the standard deviation of their corresponding PCs, the standard deviation of the respective PCs were used to normalise the PCs in order to make them unit-less. From our scree plot analysis (not shown), i.e., a plot showing the statistically significant PC modes (see, e.g., Martinez and Martinez, 2005), the first four PCA modes, which gave a cumulative variance of 96.4%, were adopted as meaningful signals representing over 95% of the total TWS variability over West Africa. The results of the principal component analysis indicate that the highest EOF loadings are observed in some parts of West Sahel and Middle Belt in the first orthogonal mode (Fig. 2).

This first PCA mode, which explains 81.3% of the variance, represents the annual variability of TWS changes in the region. The first PCA mode of the GRACE-derived TWS changes shows the strongest annual variability over Guinea and Sierra Leone and to a lesser extent over the Middle Belt region in Nigeria. Especially over Guinea, Sierra Leone, Guinea Bissau, and Liberia, the magnitude of rainfall make the regions exceptionally wet, with an average monthly rainfall ranging from 150 mm to 350 mm (see Section 4.2). Furthermore, EOF1 and its corresponding PC (Fig. 2) show an increasing trend in TWS changes over West Africa for the study period. This trend, which points towards an overall wetness in the region is discussed

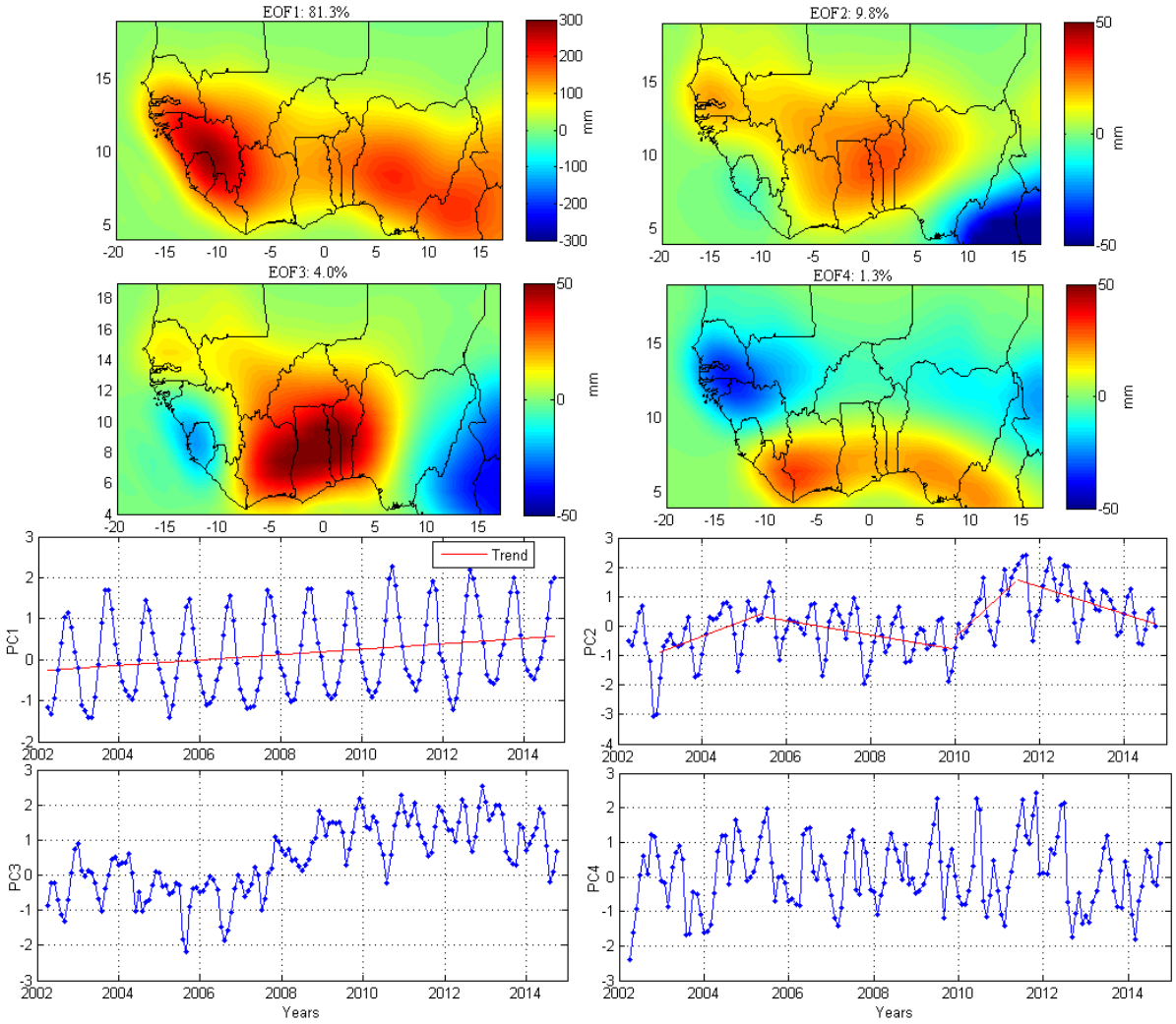

Figure 2: PCA decomposition of TWS changes over West Africa. The EOFs are loadings showing spatial patterns of variations in TWS over West Africa while the corresponding PCs are temporal variations which are normalised using their standard deviation to be unitless.

further in Section 4.5. The second EOF and its corresponding PC, which explains 9.8% of the total TWS variability, represents multi-annual variation in TWS changes over some countries in West Africa for the study period (Fig. 2). As can be seen in the corresponding EOF (i.e., EOF 2 in Fig. 2), the multi-annual variation is relatively strong over Ghana, Togo, Benin and southern Burkina Faso, the riparian countries that constitute the Volta basin. Also, over the Guinea Coast and West Sahel, a considerable multi-annual variation can be seen in the second EOF. Multi-annual variations with strong amplitudes ranging from 45 mm to 62.5 mm are observed in the Volta basin between 2010 and 2012 compared to the negative TWS change of -60 mm observed in late 2006. These multi-annual variations for example between 2010 and

2012, if related to the size of the Volta basin of approximately 407,093 km^2, will translate to $\sim$ 18.3 km^3 and $\sim$ 25.4 km^3 of water volume respectively, a rather significant amount of water when compared to Lake Volta's storage capacity of 148 km^3. These somewhat strong multi-annual changes in the TWS between 2010 and 2012 as indicated in PC2 of Fig. 2 can be attributed to increased rainfall within the period (i.e., between 2010 and 2012). This period also coincides with the period where most African lakes experienced severe flooding due to strong seasonal variations in rainfall (Moore and Williams, 2014). Also, ponding of water behind the dam might also play a critical role in the observed TWS variation in the period (this is discussed further in Section 4.5). Further, we note a phase shift (i.e., an opposite phase) in EOF2 (i.e., Fig. 2), which is due to differences in rainfall patterns in the region. For instance, Cameroon experiences an equatorial climate pattern and receives about 400 mm monthly rainfall during the wet season and peaks in October/November while over much of the Volta basin, rainfall peaks occur in July/August. The stronger loadings (i.e., when compared to the one over the Volta basin) observed in this mode in southern Cameroon is attributed to a much stronger variability in the seasonal rainfall patterns, which are also driven by West African Monsoon winds.

Since the second PCA mode explains about 10% of the total TWS variability, we further analyse the trends in the multi-annual variations of its temporal evolutions (PC2, Fig. 2) in relation to the corresponding EOF loadings over the Volta basin (i.e., Ghana, Togo, Benin and southern Burkina Faso). Our attention is particularly drawn to the Volta basin because of the huge socio-economic potential of Lake Volta and the 20 million people who depend on the water resources of the basin. To this end, we used least squares method to analyse the multiple trends observed. Instead of fitting a direct simple line to PC2 in Fig. 2, its temporal evolution was splitted and least squares method was applied to each section. That way the strong multi-annual variation will not affect the trend estimation. A linear fit (i.e., using least squares) to the second PC (Fig. 2), which represents the trend in multi-annual changes in TWS for the period investigated indicate an overall increase of 13.5 ± 4.25 mm/yr between 2003 and mid 2005 while a decrease of 6.0 ± 2.0 mm/yr was observed between mid-2005 and 2009. The period between 2010 to 2012 was quite exceptional as it experienced an increase in TWS change of about 33.5 ± 8.75 mm/yr (see, e.g., PC2 of Fig. 2). Though this period of the observed trend is short, however, it stimulates a rather strong hydrological interest regarding the possible cause of such a dramatic increase in TWS during the period (i.e., 2010-2012).

This increase in TWS could be due to the magnitude in June, July and August precipitation of that year (i.e., 2010), which made it extremely wet. After this period, a decreasing trend of about 11.5 ± 3 mm/yr is observed from 2012 up to 2014 as shown by the amplitudes of PC2. This observed negative trend in PC2 (i.e., 2012 to 2014) indicates a decline in TWS change due to declining rainfall totals over the Volta basin and its riparian countries. Overall, as shown in the next section, the rainfall trend estimate shows a decline over the Volta basin and is consistent with Ahmed et al. (2014) who also reported a decline in rainfall within this period. In a previous study, Owusu et al. (2008) had specifically attributed the decline in rainfall totals over the Volta basin to the impact of El Niño Southern Oscillation Index (ENSO) event.

The third PCA mode represents about 4% of the total TWS variability and shows again a multi-annual variation. This variation is approximately centred over Lake Volta and extends over the complete Volta basin. The strong EOF loading observed in this mode is directly over the lake and indicates multi-annual variations over the lake area. The lake (i.e., Lake Volta, which nicely fits with EOF3 of Fig. 2) had low water levels between 2003 and 2007 (Lake Volta is discussed further in Section 4.8), and had increased since the early rain onset in 2007 (see PC3 in Fig. 2). The fourth PCA mode, which accounts for 1.3% total TWS variability represents mostly a semi-annual signal due to the strong rainfall patterns at the Guinea Coast where rainfall is bimodal (i.e., two periods of wet seasons), largely influenced by intensity, and regulated by the impact of sea surface temperature (SST) (e.g., Nguyen et al., 2011; Nicholson and Webster, 2007). For instance, concerning the bimodal nature of rainfall in this area (i.e., eastern Liberia up to western and southern Nigeria), low SST anomalies lead to reduced precipitation such that rainfall decreases from about 60 cm in eastern Liberia and Nigeria to about 20 cm in Côte d'Ivoire and western Ghana (Odekunle and Eludoyin, 2008). These low SST anomalies occur between July and August and generate a *temporal dry period* or Little Dry Season (see more details in Adejuwon, 2006; Odekunle and Eludoyin, 2008) in the mid summer by supporting a condition of static stability, which hinders the development of convection, leading to low precipitation. The warm SST anomalies, on the other hand, occur in other months of the year, bringing higher precipitation before and after the *temporal dry period*, hence the bimodal rainfall in this region. Concerning rainfall intensity (i.e., strong magnitude of rainfall) over these areas, while Paeth et al. (2012) reported an abundant rainfall of 467 mm in August 2007 at Gaya station in Nigeria (i.e., 11.53°N, 3.27°E), Nguyen et al. (2011) observed that rainfall intensity between May and June in the areas near the coast varied

largely between 5.1 mm/day and 11 mm/day. This kind of intensity, number of extreme rainy days, cumulative annual rainfall, and the strong bimodal character of rainfall in this coastal region (i.e., eastern Liberia, Côte d'Ivoire, Ghana, western and southern Nigeria) are the main triggers of the observed hydrological signal in the fourth orthogonal mode of Fig. 2.

4.2. Precipitation Patterns Over West Africa for the Period 2002 to 2013

The discussion in this section focuses on the TRMM rainfall distribution over West Africa for a 12-year climatological window (i.e., 2002-2013). While mean monthly rainfall distribution within the time period investigated varied from less than 50 mm to more than 300 mm in West Sahel, the Central Sahel received less than 100 mm (Fig. 3a). Also, mean monthly rainfall distribution ranged from less than 80 mm to more than 300 mm at the Guinea Coast while rainfall in the Middle Belt region ranged from less than 100 mm to more than 200 mm (Fig. 3a). Besides the movement of the ITCZ, and the influence of atmospheric circulation features such as African Easterly Jets (AEJ), West African Westerly Jets (WAWJ), and Tropical Easterly Jet (TEJ) (see, e.g., Nicholson and Webster, 2007; Nicholson and Grist, 2001), the influence of altitude and physiographic features plays a major role in the annual and monthly rainfall distribution in the region (see, e.g., FAO, 1983). For instance, the highland areas such as Sierra Leone, Guinea, and Cameroon receive more rainfall than the surrounding lowlands in the Central Sahel (Fig. 3a).

In addition, trends in spatial precipitation patterns over the region indicate an increase between 1.5 mm/year and above 6 mm/year and a decrease of more than 4 mm/year in the sub-region (see Fig. 3b). This value, which is statistically insignificant at $\alpha = 5\%$ significance level, agrees with the findings of Marshall et al. (2012) who also observed an insignificant decreasing trend in precipitation over the region. Also, visual analyses from the temporal variations of the smoothed rainfall over West Africa show an increased magnitude of the annual signal between 2005 and 2009 (Fig. 3c). While Paeth et al. (2012) reported on flood events, which prevailed over some parts of the sub-region in 2007, this period also coincides with the period of upsurge in Lake Volta water levels (i.e., from 2006-2010), where an increase of more than 6 m was recorded. More discussion on this item will be provided in Section 4.8. Also, reports from the World Meteorological Organization in 2012 indicated that above normal rainfall resulted in flood events in south eastern Mauritania, Mali, Senegal, northern Burkina Faso, Lake Chad basin in Niger, Nigeria and Cameroon (WMO, 2013).

Despite this apparent rainfall intensity that culminates in serious flood events, the observed increase in linear trend of the spatially averaged rainfall over West Africa for the entire period (not shown) is statistically insignificant. This is consistent with Panthou et al. (2012), who noted that, despite the intermittent torrential rains, and floods in the region, dry conditions still persist, since rainfall average in recent times is still lower than in the wet periods of the 1950's and 1970's. However, concerning the relative wetness and flood incidence that have been reported in the region, the strong variability in the intensity of the annual cycle of West African Monsoon rainfall might be responsible for the occasional floods and relative wetness seen in the region. For instance, while findings in Paeth et al. (2012) suggest that the above normal rainfall in August 2007 induced by ENSO event was responsible for the flood event in some parts of the river basins across the region, other studies have reported strong rain seasons near the Guinea coast around the June-September period (see, e.g., Diatta and Fink, 2014; Nguyen et al., 2011). The seasonal variation of rainfall is discussed in subsequent sections.

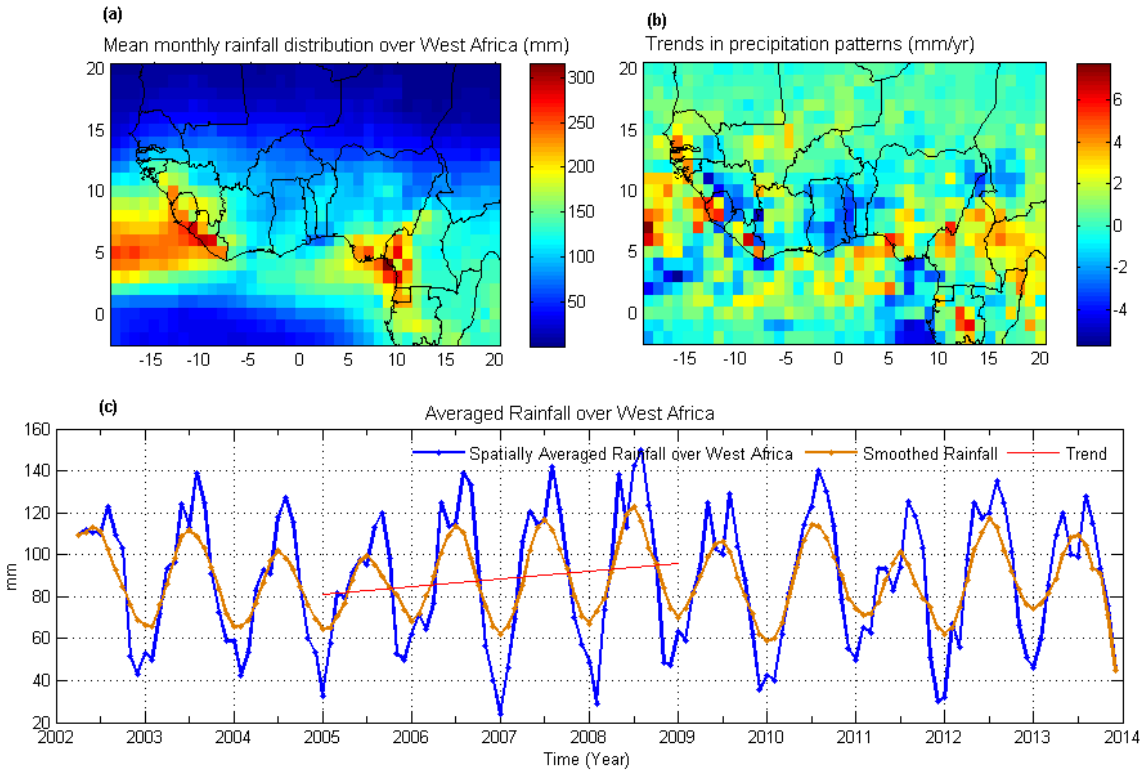

Figure 3: Rainfall distribution and trends over West Africa, (a) Mean monthly rainfall distribution for the period 2002-2013, (b) Trends in rainfall, and (c) Temporal variations of rainfall (2002-2013).

4.3. Spatio-temporal Variability of Rainfall

From the PCA results, the cumulative variability explained by the first four most dominant modes is approximately 72.2%. Since the size of the spatial domain determines the performance of PCA (Westra et al., 2010), the variance explained by the first four most dominant modes can be improved if the analysis is limited to the sub-regions within the study area (i.e., if the oceans are masked). However, since the West African Monsoon (WAM) system conveys moisture from the surrounding ocean, understanding the spatio-temporal patterns of rainfall along the oceans as well will improve our knowledge of land-ocean dynamics in the region. In our analysis, the highest loadings from the first EOFs, representing 49.5% of the total variability, are concentrated around West Sahel, Central Sahel, and some parts of the Guinea Coast (Fig. 4). This orthogonal mode describes the sub-regions with considerably strong annual rainfall variability. The second PCA mode, which explains 12.2% of the total variability, represents semi-annual rainfall patterns mostly over the ocean but also extending to the Guinea coastal region. The third and fourth orthogonal modes and their corresponding PCs, which explain 6.2% and 4.3% of the total variability, respectively, represent a combination of multi-annual and seasonal variability of rainfall in the region. These variations (i.e., PC1, PC2, and PC3 of Fig. 4) are largely due to annual rainfall cycles, circulation features, and influence of ocean warming and climate teleconnections in the Sahel and Guinea coast region (see, e.g., Diatta and Fink, 2014; Paeth et al., 2012; Lebel and Ali, 2009).

These rainfall structures and patterns over West Africa suggest the dominance of annual and semi-annual variability in West African Monsoon rainfall, and a progressive shift in the semi-annual cycles of rainfall from the Guinea Coast to the Central Sahel (see, e.g., Barbe et al., 2002; Lebel and Ali, 2009; Diatta and Fink, 2014). This annual variability can be linked to changes in August and September rainfall (Nicholson, 2014). Also, the sea surface temperature (SST) of the eastern Atlantic and the role of the Atlantic Cold Tongue (ACT), which regulates the intensity and timing of coastal rainfall in spring, have been largely associated with the dominance of inter-annual and seasonal variability of rainfall in these sub-regions (Nguyen et al., 2011). In addition to the impact of SST on seasonal and inter-annual rainfall, other climate indices such as the Atlantic Multi-decadal Oscillation (AMO), Atlantic Meridional Mode (AMM), and Madden Julian Oscillation (MJO) have been identified to have positive correlation with rainfall patterns in the region (see, Diatta and Fink, 2014; Nicholson, 2013). However, the PCA method could not represent any of such patterns in either of the EOF

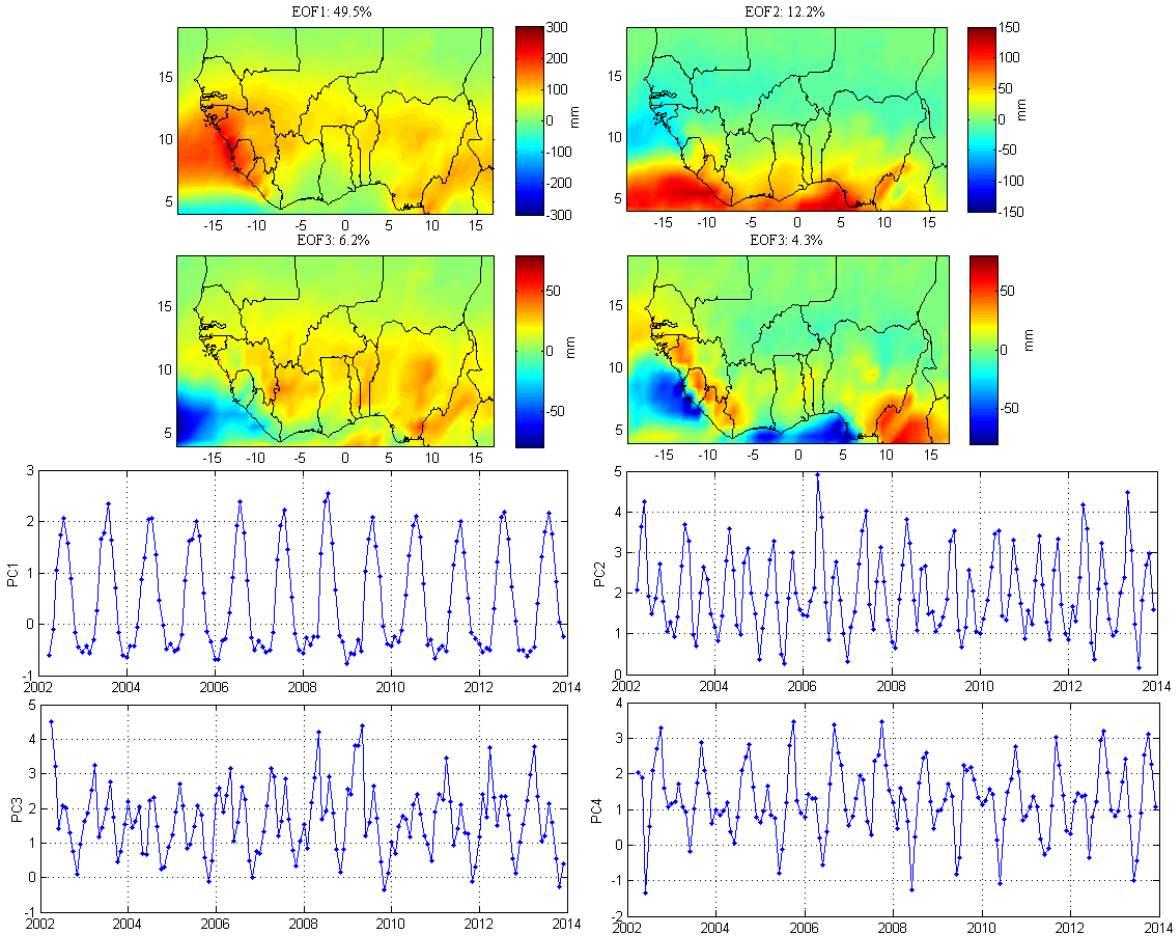

Figure 4: PCA decomposition of TRMM precipitation over West Africa. The EOFs are loadings showing spatial patterns of variations in precipitation over West Africa while the corresponding PCs are temporal variations which are normalised using their standard deviation to be unitless.

loadings or the corresponding principal components. This weakness in the PCA method, which arises due to the orthogonality of its temporal and spatial components, will be addressed in future studies by investigating other higher order statistical methods such as Varimax rotation and independent component analysis (ICA), which maximises regional phenomena (e.g., Westra et al., 2010; Common, 1994).

Further, there were no significant linear trends in the principal components as determined by a least squares fit (not shown). Considering the observed increase in the annual TWS temporal patterns (PC1, Fig. 3), it is normal to assume a linear relationship between rainfall and change in storage over time. However, over Guinea and parts of West Sahel, such relationships might not be completely linear as annual variation in discharge for example can only be partly explained by the annual variation in precipitation (Verschoren, 2012). This

non-linear relationship can be attributed to variations in the type and morphology of rivers, geology, physiography, vegetation, soil type, ponding of water behind dams and reservoirs, and the catchment extent amongst others. We provide more discussion on this in Section 4.5. However, the lack of a significant positive trend in rainfall as observed in the temporal evolutions of PC1 in Fig. 4 suggests a fairly stable climatic regime for the whole study area (see also, Fig. 3b) regardless of occasional changes in intensity and increased inter-annual and seasonal variability in rainfall. This position is consistent with Giannini et al. (2013) who reported that increased daily rainfall intensity is a contributing factor to the perceived rainfall recovery in the region. However, a decline in rainfall mostly over parts of the West/Central Sahel and Lake Volta basin is observed (Fig. 3a and b). There is a tendency towards aridity in those regions, particularly over the Volta basin where Owusu et al. (2008) had previously reported that the declining rainfall totals, triggered by the warm phase of ENSO, are the main cause of the decline in Lake Volta water levels in the Volta basin. In view of this result, the region's susceptibility to drought conditions might increase as reported in Asefi-Najafabady and Saatchi (2013).

4.4. Analysis of Trend and Seasonal Variations of Precipitation and TWS

The seasonal cycle of precipitation and changes in TWS were estimated by spatially averaging monthly values over the study period. While the averaged values for the rainfall seasonal windows shows maximum rainfall in the July-August-September period, the change in TWS shows maximum seasonal variations in the October-November-December period (Figs. 5a and 5b). On the other hand, the mean monthly rainfall shows a peak in August, while the mean monthly change in TWS for the study period shows a peak in October (Fig. 5c). Apparently, this shows that TWS lags behind rainfall in the region by approximately two months. To further ascertain the time response of TWS to rainfall, the temporal evolutions of the dominant TWS and rainfall orthogonal modes (i.e., PC1 Fig. 2 and PC1 Fig. 4) clearly indicate a two month lag between TWS and rainfall when their annual peaks are compared (i.e., while rainfall peaks in August, TWS peaks in October). On the whole, the analysis of our rainfall grouping (i.e., the different seasonal periods) is consistent with the classification of major West African annual rainfall settings outlined in recent studies (see, e.g., Druyan and Fulakeza, 2015; Thorncroft et al., 2011). That is, for instance, our Jan-Feb-March period describes the oceanic phase when the rainbelt is large with maximum precipitation values just north of the

559 equator; April-May-June refers to the coastal phase with peak rainfall values around coastal
560 regions within the gulf of Guinea, i.e., Guinea Coast; while the July-August-September period
561 describes the Sahelian phase where maximum rainfall is established around latitude 10N (see
Figs. 5a and 5b).

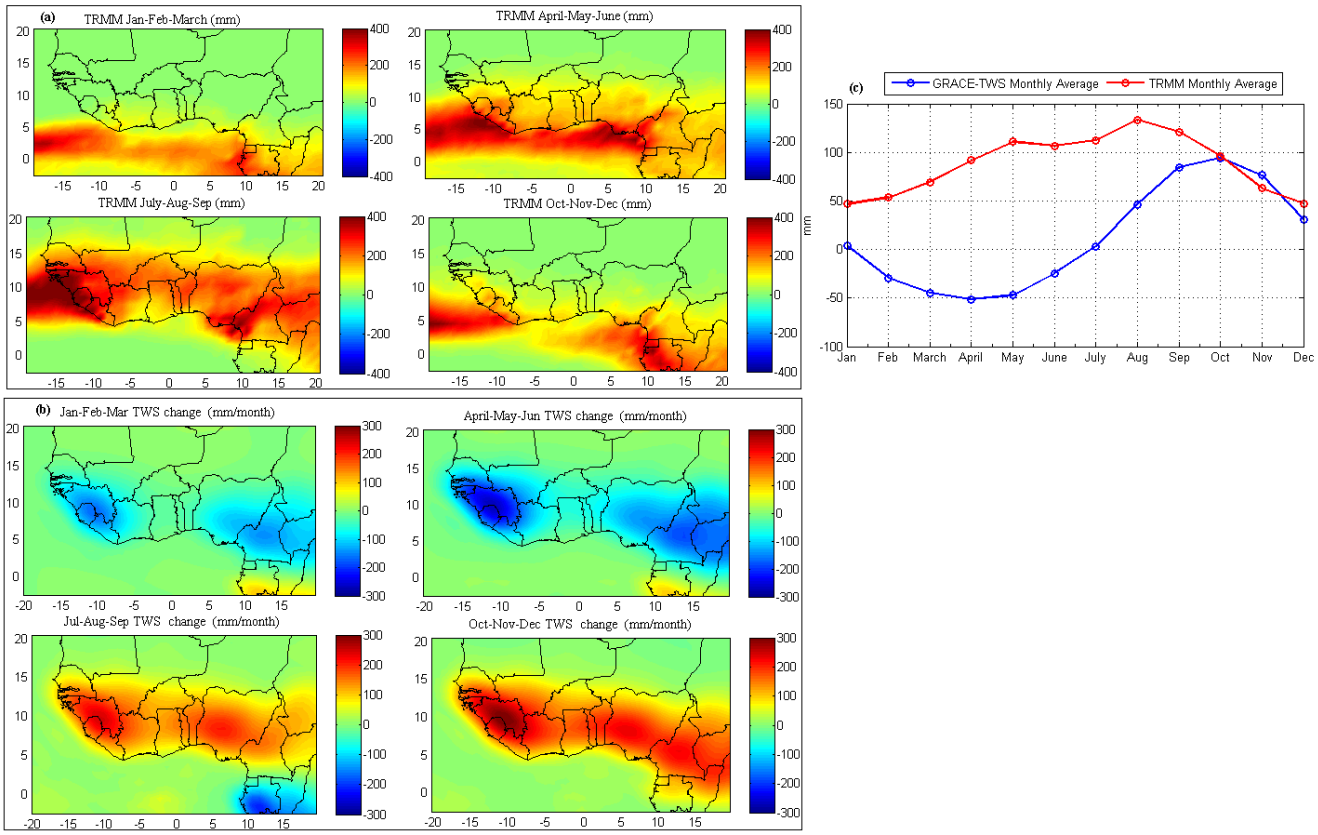

Figure 5: Seasonal cycles of GRACE derived TWS changes and precipitation; (a) TRMM averaged values for the seasonal periods, (b) GRACE-TWS averaged values for the seasonal periods, and (c) mean monthly rainfall and TWS change over West Africa.

562

563 From the TWS variability index, the years 2002 to 2006, and early 2007 are indicative
564 of dry years, while the year 2010 and beyond was quite wet (Fig. 6a). The rainfall shows
565 dry conditions in 2004 to 2006, wet conditions in 2010, extreme conditions in 2011, and near
566 normal conditions in 2009 and 2013 (Fig. 6b). One relevant observation made from the rainfall
567 variability index is that the dry periods of 2004 to 2006 correspond to the dry periods observed
568 in the TWS index of variability. This implies that rainfall is a major contributor to the
569 hydrological flux in the region, and that change in precipitation patterns as observed in the
570 region is likely to be the most significant driving factor for the surface mass variations, hence
571 the dominant patterns observed in TWS changes. The PCA results (especially the dominant

patterns) for both GRACE-TWS and rainfall confirms this hypothesis (see Sections 4.1 and 4.3). Further, our analysis of TWS variability index in terms of trends and seasonal variability shows that the region experienced water deficit between 2002 and mid-2007 (Fig. 6b). This perspective is very similar to results of Asefi-Najafabady and Saatchi (2013), who reported that West Africa experienced strong negative water storage anomalies between 2005 and 2007. Though our analysis of rainfall variability commenced in 2002, we infer based on previous studies (e.g., Nicholson, 2013; Panthou et al., 2012) that the observed water deficit between 2002 and 2007 is an extension of the drought period in the 90s, which continued unabated despite the perceived rainfall recovery. While the impact of the 1991 and 1997 El Niño events, which caused low rainfall in the region, are noted (e.g., Nicholson and Webster, 2007; Owusu et al., 2008), Nicholson (2013), specifically pointed out that the relative recovery in rainfall over West Africa was not all encompassing, and that the mean annual rainfall within the period (i.e., 1990 to 2007) is significantly not different from the mean of the acknowledged drought period.

However, from our analysis of changes in TWS averaged over West Africa (i.e., after removing the harmonic components), there seems to be a relative increase in water availability in recent times (i.e., the period between 2012 and 2014). Since Fig. 6a shows wet conditions between 2012 and 2014, we fitted a linear trend to the GRACE-derived TWS for the same period in order to understand TWS trend in recent times, which is useful for planning and management. While the least squares fit for the period between 2012 and 2014 for the averaged GRACE TWS changes after removing annual and semi-annual components shows a significant increase of 7.47 ± 3.98 mm/yr in the linear trend (Fig. 6c), the averaged TWS anomalies over West Africa (i.e., over land) for the study period show a linear increase of 6.85 ± 1.67 mm/yr (Fig. 7), which is statistically significant at 95% significance level. This increase in TWS trends over the region, could be attributed to a large water surplus from prolonged wet seasons and lower evaporation rates in coastal West Africa (i.e., Guinea Coast and some parts of West Sahel), which remarkably increases the water storage and inundated areas along the coastal catchments that sustain the dry season river flow (Ojo et al., 2004). In view of this recent trend in TWS change, it is expected that crop development, moisture conservation, and soil fertility for some parts of the region might be significantly improved. In Section 4.5, we provide further details to highlight the non-linear behaviour observed in the temporal evolutions of the annual signals of our PCA results for TWS and rainfall as indicated

in PC1 of Fig. 2 and 4, respectively.

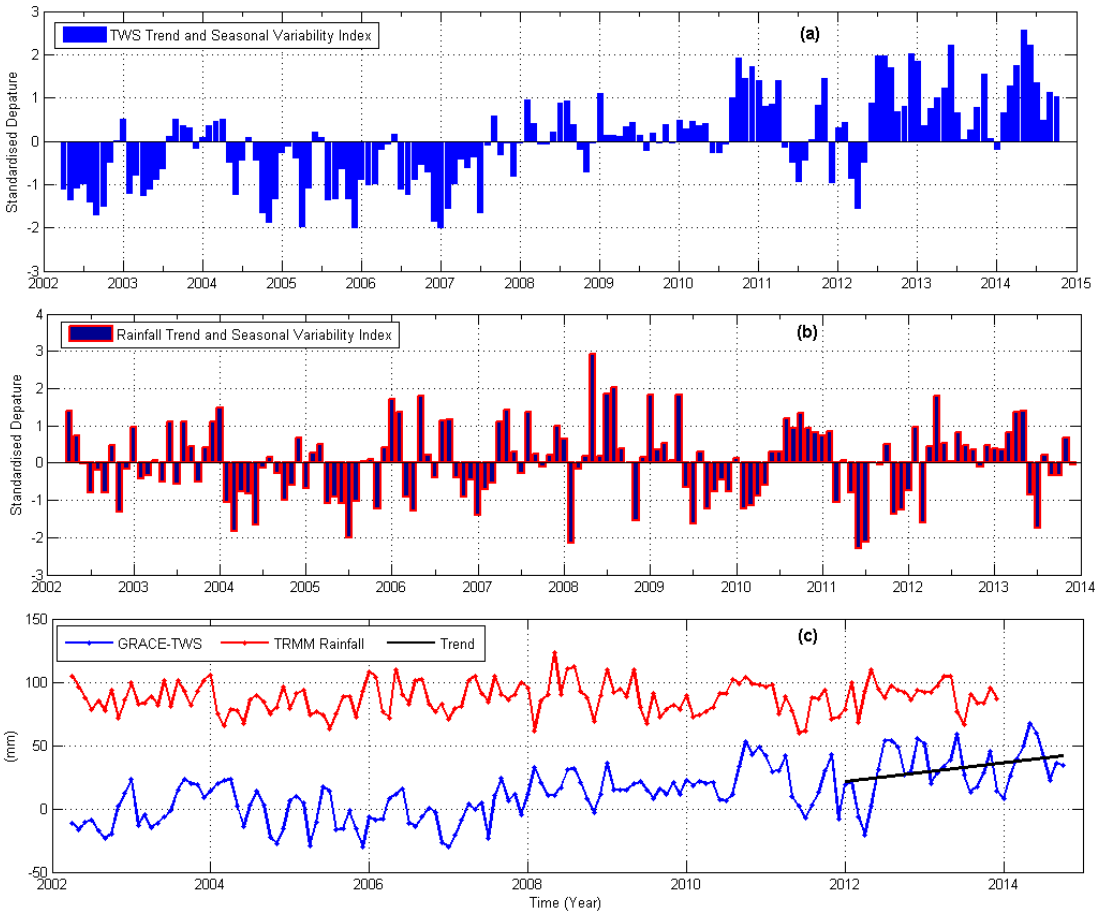

Figure 6: Variability Index after removing annual and semi annual components. (a) GRACE-TWS variability index, (b) TRMM rainfall variability index, and (c) Least squares fit of TWS anomalies for the period 2012-2014 (i.e., not standardised).

4.5. The hydrology of the Fouta Djallon Highlands

The Fouta Djallon Higlands (FDH) comprises chains of mountainous landscapes mostly in Guinea and extend into countries such as Sierra Leone, Guinea-Bissau, Senegal, Mali, Côte d'Ivoire and Liberia (Verschoren, 2012). The highlands, which are small watersheds and sources to major West African rivers (e.g., River Niger, Senegal, Gambia, and Mano) have been labeled the *water towers* of West Africa. These rivers provide drinking water, irrigation and hydroelectric power to millions of people who make their homes in the catchment. Our interest in FDH is due to the strong dominant spatio-temporal behaviour observed in our PCA results for TWS and precipitation. While the annual variability of TWS especially in Guinea (PC1 Fig. 2) shows a steady increase in water storage change, annual variability of precipitation

shows no obvious significant increase in the same area (PC1 Fig. 4). The temporal evolution of PC1 in Fig. 2 indicates a significant rise of 20.2 ± 5.78 mm/yr in Guinea while no significant increase was observed in rainfall. The hydrology of these watersheds (i.e., FDH) is largely controlled by components of the hydrological cycle such as precipitation, runoff, and recharge. The water balance model can be written as

$$P = E + Q + \delta S, \tag{7}$$

where P, E, Q, and δS are precipitation, evapotranspiration, runoff, and change in storage respectively. The storage variable, that is the runoff deficit variable, R_D, can be defined as

$$R_D = P - Q, \tag{8}$$

where the runoff deficit R_D is the amount of water, which is stored in watershed, evaporated, or water lost through the process of transpiration (i.e., the yearly water availability). For the FDH, vegetation has not been modified and both temperature and evaporation are relatively low in these areas especially during rainy season (Verschoren, 2012). Hence, it is reasonable to assume that no change has occurred in transpiration within the period. Increase in R_D implies increase in the volume of water not involved in surface runoff. This quantity, which is assumed to have increased over time, represents the aquifer storage. With precipitation spreading over 8-12 months of every year, lack of significant change in evapotranspiration, and huge groundwater potentials, in addition to very high aquifer productivity as shown in MacDonald et al. (2012), the aquifer storage is likely to increase despite the lack of positive trend in rainfall within the studied time period . The apparent increase in temporal patterns of annual TWS signal (PC1 Fig. 2), which coincides with the somewhat limited alimentation due to lack of significant positive trend in rainfall, is consistent with the findings of Verschoren (2012) who observed over the FDH a non-linear relationship where a higher increase in discharge was inconsistent with observed precipitation. Comparatively, the amplitudes of annual rainfall observed in PC1 of Fig. 4 indicate that the years 2003 and 2006-2008 have relatively stronger annual peaks. Recently, McSweeney et al. (2010) reported that the variations in the latitudinal movements and intensity of the ITCZ from year to year can cause large inter-annual variability in the wet season rainfall leading to 1000 mm of monthly rainfall at the east coast of Guinea. This kind of variability, besides increasing the inundated areas in the catchment, will largely increase the amount of water stored in the watersheds, given that evaporation is generally low

during the wet seasons in Guinea. Further, besides the high precipitation amounts of more than 3000 mm annually, Guinea is a region with heavy discharge, huge base flow and abundant water resources. For instance, the quantity of water entering Mali from Guinea is estimated at 40 km^3/yr, greater than the quantity entering Nigeria from Niger, which is estimated at 36 km^3/yr (FAO, 1997). In south-west Guinea where the EOF loadings are relatively strong, the average annual peak rainfall in the wet season ranges from $\sim$ 687.5 mm/yr between 2006 and 2008 to $\sim$ 550 mm/yr between 2010 and 2013 when jointly derived from the PC/EOF (PC1/EOF1, Fig. 4). With sub-regions such as Boke, Boffa, and Forecariah (i.e., local areas in Guinea where these rainfall amounts are observed), which lie along the coast in Guinea and covers a total surface area of $\sim$ 40500 km^2, these rainfall amounts will give average annual water volume (i.e., in the wet season) estimated at 27.8 km^3/yr and 22.3 km^3/yr for the 2006-2008 and 2010-2013 peak periods respectively. This estimated amount of water volume excludes that of the northern and extreme western regions of Guinea where our PC/EOF method estimates average annual peak rainfall of 375 mm/yr and 300 mm/yr for the two periods, respectively. Since about 40 km^3/yr of water leaves the country (i.e., Guinea), R_D increases over time despite lack of positive trend in rainfall, hence the increase in TWS trend observed over Guinea in PC1/EOF1 of Fig. 4. Also, note that our rainfall estimate here is for the peak rainfall only, which is more like the average rainfall in August with respect to the mean of 2002-2013. Considering a minimum of eight months of significant precipitation in south-west of Guinea, the water balance will apparently indicate a surplus regardless of stability or lack of positive trend in rainfall.

Moreover, in a related study, a similar relationship of increased TWS not being consistent with precipitation trends was recently reported by Ahmed et al. (2014) in a continent-wide study. The study observed an increase of 15.35 ± 0.79 mm/yr and 16.68 ± 1.09 mm/yr in Okavango and Zambezi basins, respectively with no obvious significant increase in precipitation. The increase in TWS was attributed to the increased size of inundated areas of the basins and the cyclical nature of recurrent floods amongst other factors. Further, human activities such as building of dams and reservoirs will impound surface water in man-made lakes from the dams upstreams, inducing infiltration and consequently leading to increase in recharge from the lakes to groundwater. This example was reported for the Lake Volta basin in the region where an increase of 14.41 ± 1.02 mm/yr was observed for the period between 2003 and 2012, despite lack of a significant trend in rainfall for more than a period of 10 years (see, Ahmed

et al., 2014). The observed TWS over the basin (i.e., Lake Volta basin) was attributed to ponding of water behind the dam, which is also evident in the apparent increase of 7 m in Lake Volta water levels as shown in Section 4.8 (Fig. 12a). Also, over the Niger basin (which includes Guinea, Nigeria, Mali, and countries with dominant patterns in TWS as observed in the PCA result, i.e., PC1 Fig.2), Ahmed et al. (2014) also observed an increase of 6.31 ± 0.36 mm/yr in TWS for the period 2003 to 2012, which is somewhat consistent with the trend of 6.85 ± 1.67 mm/yr in observed TWS in our study. While a detailed study will be required to understand the role of land use in the hydrology of the FDH, Favreau et al. (2009), had shown a rising water table of about 4 m between 1963 and 2007 in southwest Niger despite about 3% deficit in rainfall from 1970 to 2007. This paradoxical relationship, which is similar to the behaviour of our hydrological time series (i.e., rainfall and TWS) as observed in Guinea and the surrounding areas, was attributed to a change in landuse pattern.

Furthermore, since West Africa and the continent at large were worst hit by droughts in the 1980's (especially the Sahel), we also speculate that the recovery in the 1990's, which was not all-encompassing could account for the inconsistent trends between TRMM based precipitation and TWS, given that the huge aquifers of the Guinea region is still filling up. GRACE measures vertically integrated water storage from catchment stores (i.e., aquifer, soil moisture, etc.), any form of increase from these catchment stores will be apparent and captured by GRACE, unlike rainfall were transition periods from dry to wet might not be very obvious due to the impact of the previous extreme and frequent dry periods as in the case of the Sahel region. Generally, the water resources of West Africa are complex as seepages and evaporation are said to have triggered large reductions in runoff in the inner delta of Mali (FAO, 1997) in addition to the impact of land use change, human influence, and climate variability (see, e.g., Ahmed et al., 2014; Favreau et al., 2009; FAO, 1997). Anthropogenic effect on changes in TWS over West Africa can be modelled from Water Gap Hydrological Model (WGHM) and this can be explored in future studies.

4.6. Relationship between GRACE-TWS, GLDAS-TWS, and TRMM

The cross-correlation result shows that TRMM rainfall leads GRACE-TWS changes in most parts of the region with a maximum phase lag of two to three months (Fig. 8c, see also Fig. 6c). This is consistent with the results in Section 4.4. Also in this study, the Pearson correlation coefficient was employed to examine the relationship between GRACE/TRMM and

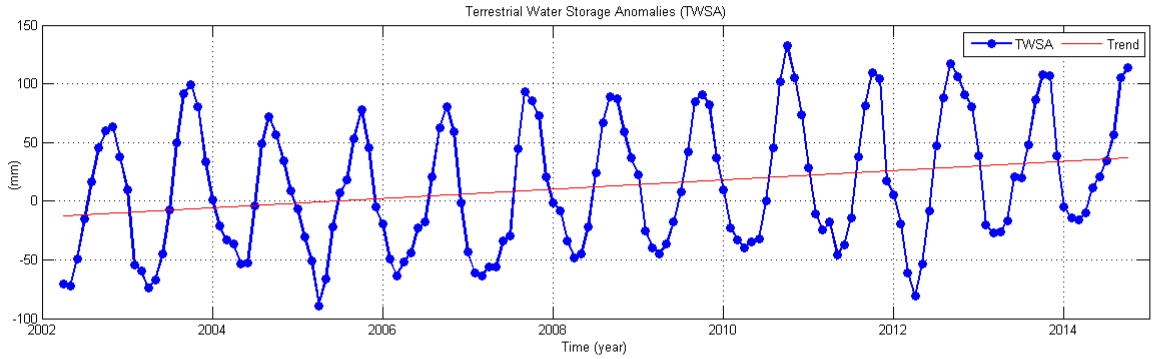

Figure 7: Trend in TWS anomalies over West Africa for the period 2002-2014 (i.e., without removing the harmonic components). The trend is also clearly visible in PC1 of (Fig. 2)

GRACE/GLDAS total water storage contents (TWSC) at 95% significance level. Prior to this analysis, the gridded TRMM rainfall product was resampled to a 1° x 1° regular grid as the GRACE-derived TWS.

The result from TRMM rainfall product and GRACE-TWS comparison shows a high correlation in some parts of West Sahel and Middle Belt regions (e.g., Guinea) while weak correlation is observed in most sub-regions of West Africa (e.g., Niger, Burkina Faso, etc.) (Fig. 8b). The observed correlation in these regions is due to the presence of a strong annual signal as can bee seen in the corresponding EOF1 of TWS (Fig. 2) and TRMM (Fig. 4). While the high correlation in West Sahel apparently defines the impact of rainfall on changes in TWS of the sub-region, the weak correlations could be the unexplained impact of water storage in the region's tropical forest. GLDAS-TWSC on the other hand, has a good correlation with GRACE-TWS for most parts of the region except for some locations in the upper Central Sahel and some parts of the Volta basin (Fig. 8a). The poor correlation of GLDAS-TWSC in those areas might be due to anthropogenic influence and probably intensified land surface processes, which the model could not account for (e.g., James et al., 2007). For example, water withdrawals and increased surface runoff due to change in land cover could possibly contribute to weak correlations in these areas.

Moreover, as mentioned earlier in this study, lack of in-situ data for calibration and parameterisation of the GLDAS model outputs could largely be responsible for the poor correlation between GLDAS-TWSC and GRACE-TWS in these locations. Since GRACE TWS observa-

tions have been previously compared with GLDAS over the Volta basin and Southern Mali (see, e.g., Henry et al., 2011; Ferreira et al., 2014), the poor correlation of GLDAS in some areas could not have emanated from GRACE TWS. This assumption follows the numerical results of Henry et al. (2011), where observed monthly groundwater-storage variability in the region correlated strongly with monthly GRACE TWS changes whereas the timing of GLDAS-derived soil moisture was not well predicted. concerning the weak correlation between TRMM precipitation and GRACE-derived TWS, some anthropogenic contributions that impact on land surface conditions might play a major role. For instance, the loss of 21,342 hectares of

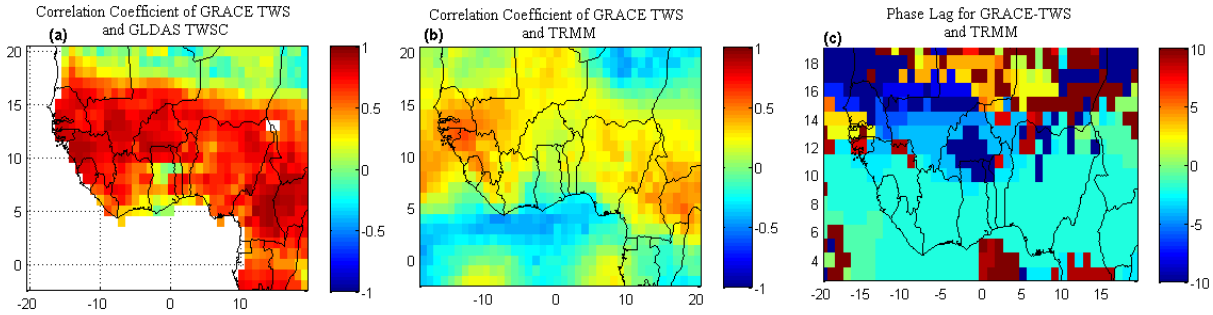

Figure 8: Correlation analysis and time lag with maximum correlation using TRMM precipitation and GRACE-TWS. (a) Correlation between GRACE-TWS, and GLDAS TWSC (b) Correlation between GRACE-TWS, and Rainfall and (c) Time lag with maximum correlation for GRACE-TWS and TRMM precipitation in months.

mangrove vegetation in the lower Niger Delta of the Middle Belt region between 1986 and 2003 due to urbanisation, might introduce some imbalance in the hydrological routines of the region (James et al., 2007). Future studies with focus on the land surface processes such as increased potential evaporation loss during the dry season, the contributions of land surface conditions, and historical land use/land cover activities in some parts of West Africa might provide some insight and clarity as to the cause of the weak correlations between GRACE-TWS and TRMM rainfall products in these sub-regions.

However, the high correlation between TWSC output from GLDAS and GRACE TWS in most parts of West Africa suggests that hydrological monitoring and climate research in these areas of West Africa can be reliable even with the use of hydrological models (i.e., outputs from GLDAS). Furthermore, the GRACE-derived TWS and the TWSC from GLDAS were averaged over land areas in the region. Their temporal variations both indicate annual cycles with similar high and low peaks that correspond to rain and dry seasons in the region (Fig. 9a). While GRACE-TWS and the TWSC from GLDAS show peaks that correspond to the same time

period, however, TWS output from GLDAS is underestimated for the region. Our conclusion here is similar to findings from a related study in southern Mali, where predicted soil moisture from GLDAS was poor (i.e., underestimated) (Henry et al., 2011). The poor prediction of soil water storage using GLDAS in the region corroborates our account of GLDAS underestimation of simulated TWS in the present study. However, the regression fit between the two variables, which shows a coefficient of determination (R^2) of 0.85 indicates that most parts of the region have been well modelled in terms of trends and variability (Fig. 9b).

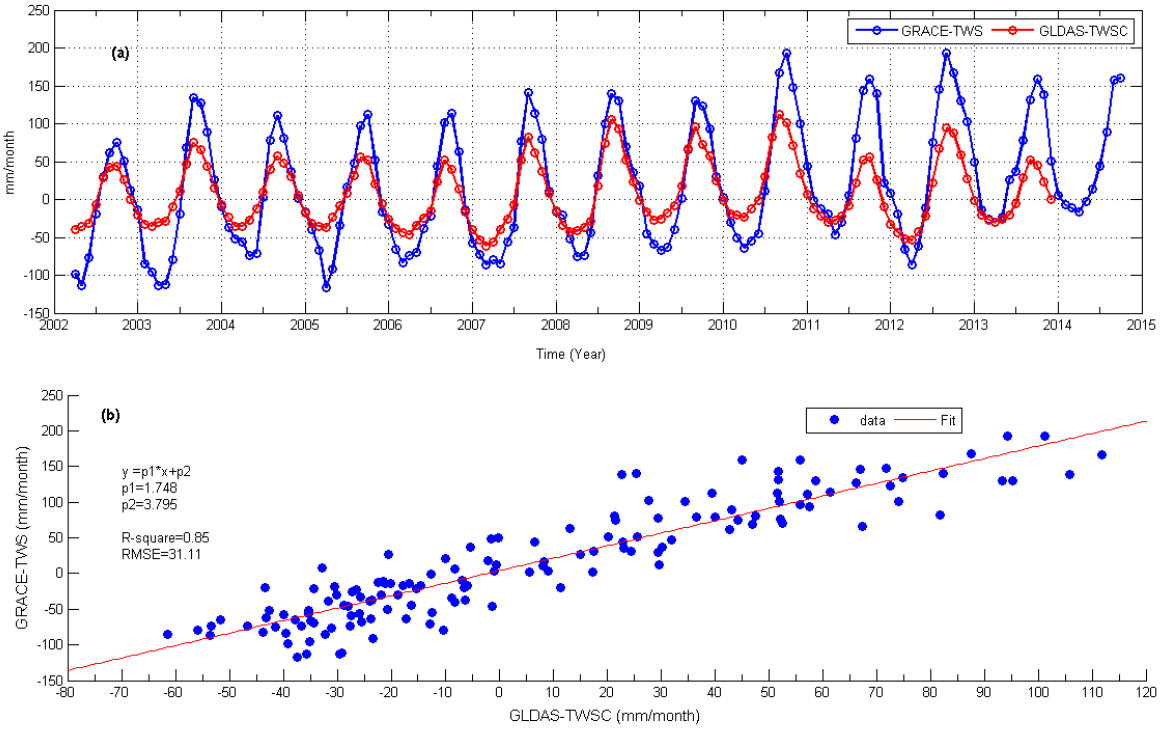

Figure 9: (a) Temporal variations of GRACE-TWS and GLDAS TWSC and (b) Regression fit on GRACE TWS and GLDAS TWSC.

4.7. Modelling TWS Anomalies and Rainfall over West Africa

The MLR analysis was applied in order to further explore the relationship between TWS changes and precipitation patterns over West Africa. Comparatively, MLR allows the test of statistical significance on the spatio-temporal patterns as opposed to PCA that divulges the dominant spatio-temporal patterns (Rieser et al., 2010). Here, we compare the results of MLRA of TWS and rainfall, especially their annual amplitudes, semi-annual amplitudes, and trends. We point out briefly that since seasonality induces the largest signals in hydrological quantities, our intent here is also to examine the capability of MLRA in mimicking TWS and

rainfall using linear trend, annual, and semi-annual signals. While their annual amplitudes are quite similar, the semi-annual signals show some disparity especially in rainfall patterns along the Central Sahel (Figs. 10 and 11). This probably suggests that the incoming rainfall leaves the region through some intensified outgoing hydrological fluxes and processes such as evapotranspiration, and surface runoff from major rivers. For instance, Marshall et al. (2012) showed how evapotranspiration correlates strongly with precipitation in the region. On the other hand, trends of both rainfall and GRACE-derived TWS are different. While higher positive trends in TWS are concentrated around the Volta basin and the Lake Volta area (Fig. 10), precipitation trends over the same area show both low/high negative and positive patterns (Fig. 11). The strong hydrological signals from the Volta basin as a result of the presence of Lake Volta largely accounts for the observed positive trends in TWS. From the coefficient of determination (Figs. 10 and 11), the multi-linear regression (MLR) model approximates TWS and rainfall quite well by using trend, annual, and semi-annual signals only. Considering the performance of MLR for rainfall in this study, similar conclusions to those of Diatta and Fink (2014) can be reached. That study concluded that using MLRA, the West African Monsoon rainfall can be better predicted especially when combined with teleconnection indices. However, as indicated in their RMSEs and coefficients of determination, some parts of West and Central Sahel are poorly modelled in the two products (see Figs. 10 and 11). Furthermore, since the coefficient of determination for the TWS simulation in the West Sahel, Guinea Coast, Middle Belt and some parts of Central Sahel show a good fit, the change in TWS for these sub-regions can be predicted quite well.

4.8. Lake Water Levels in West Africa

In order to understand the seasonal fluctuations of surface waters (i.e., lakes), the annual and semi-annual components of fluctuating water levels from Lake Volta, Lake Chad, and Kainji dam for the period 1993 to 2013 were removed using the least squares approach. The results show that Lake Chad and Kainji dam were dominated by annual and semi-annual variations while Lake Volta has a considerably strong annual signal (see Fig. 12a). The Lake Chad water level reduced by about 90% during the intense drought of 1968 to 1974, and its surface area had since shrinked from 24000 km^2 in the 1950's to about 1800 km^2 in the 1980's (Okonkwo et al., 2014; Wald, 1990). Generally, the declining Lake Chad surface area has been attributed to agricultural activities (i.e., water use for irrigation) and the impact of climate

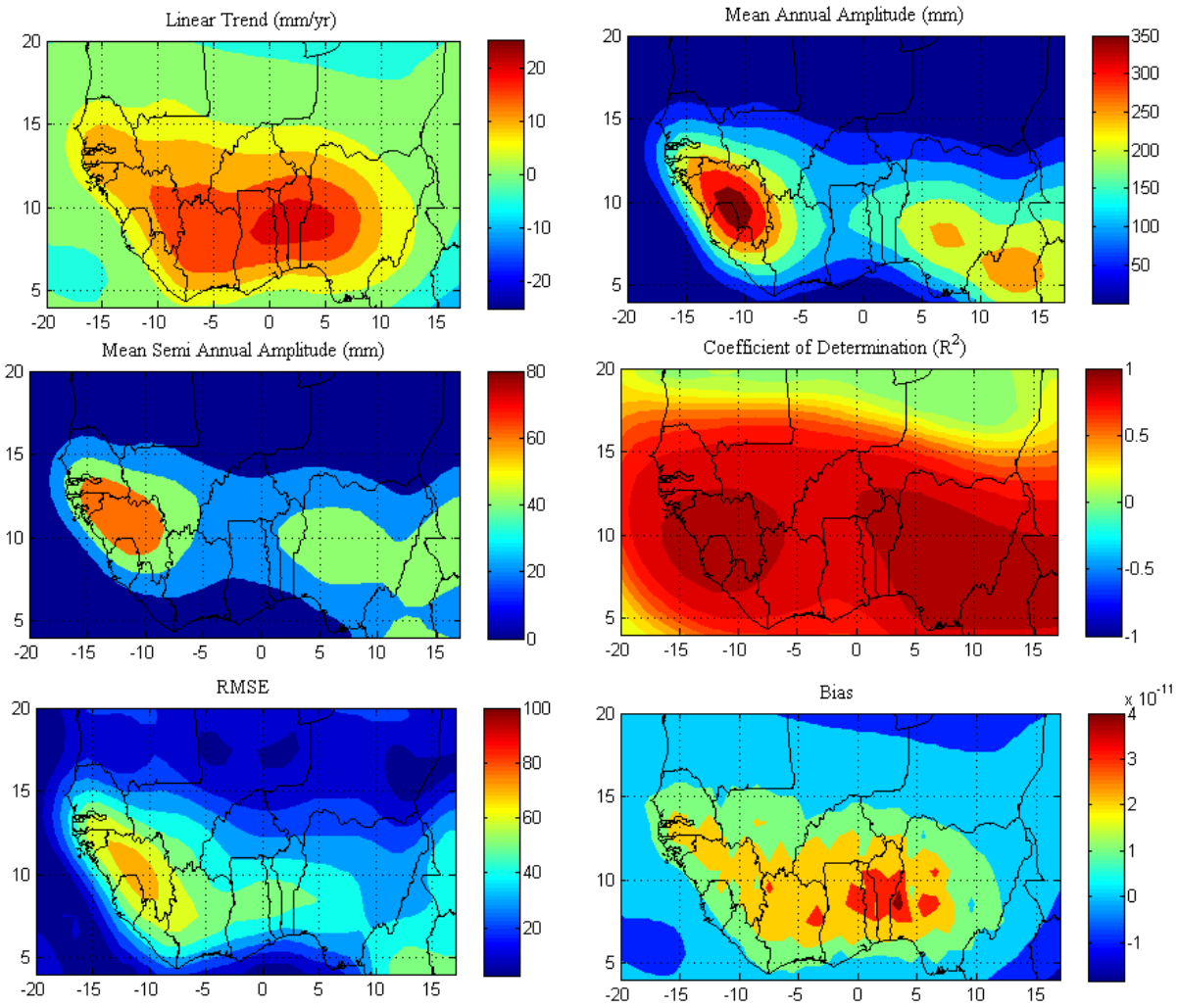

Figure 10: MLR analysis of GRACE-TWS.

variability (e.g., Coe and Foley, 2001; Gbuyiro et al., 2001).

With strong annual variability, the minimum water level of Lake Chad is observed between May/June (see Fig. 12a). Wald (1990), observed that the Lake Chad water level decreases in November and later rose to its maximum in January as a result of inflow from Logone - Chari - El Beid rivers. With a clearly marked annual fluctuation, observed minimum water levels and less pronounced annual signals of Lake Chad between the period 2004 and 2007 are indicative of dry periods induced by low summer rainfall in that sub-region while an increasing trend is also observed in maximum water level in recent years (i.e., 2010-2013) (Fig. 12a), which is consistent with increased rainfall.

For Lake Volta, its temporal variation (i.e., from 2006 to 2014) is similar to the third

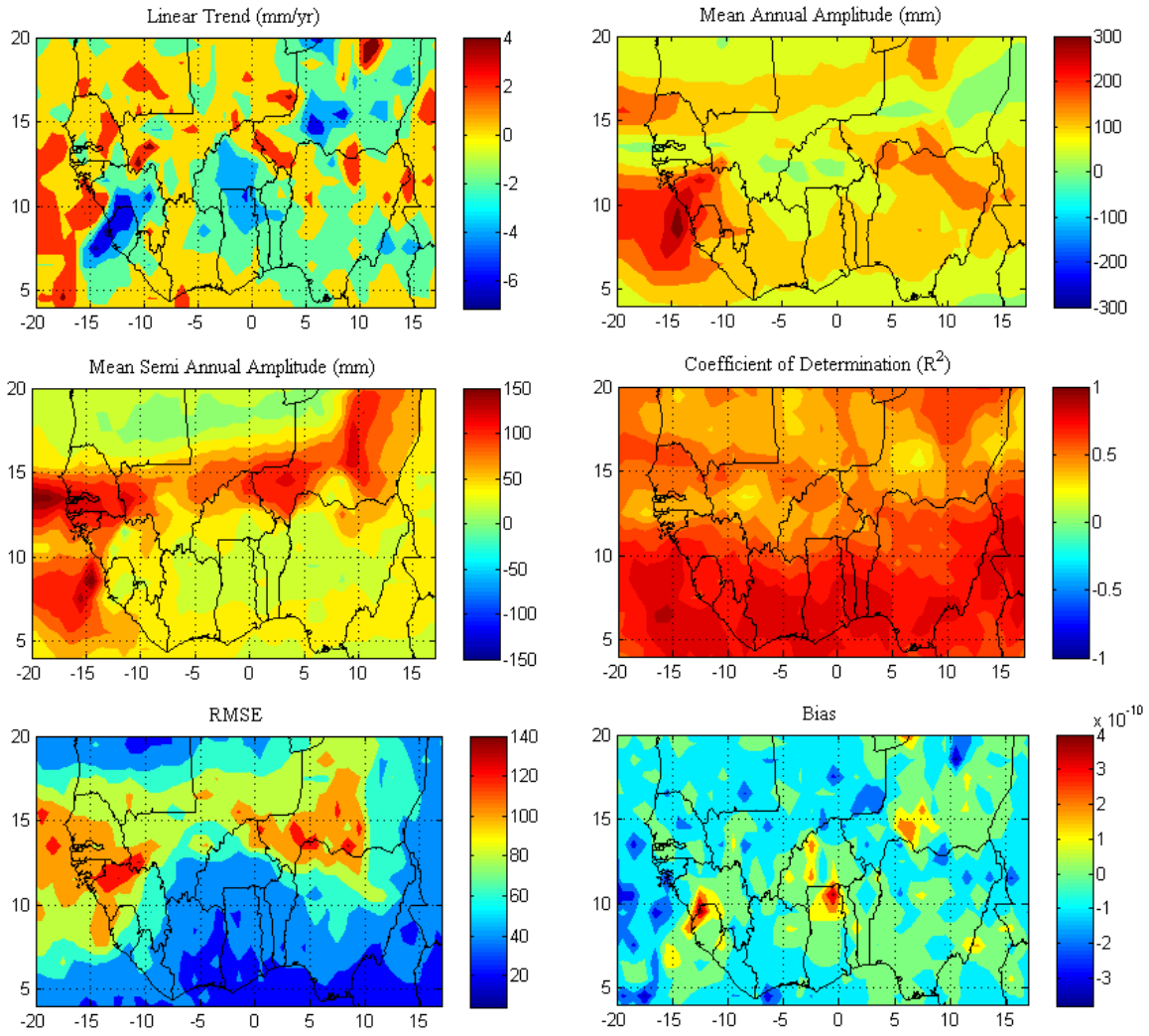

Figure 11: MLR analysis of TRMM rainfall.

principal component from our GRACE-TWS PCA, which represents multi-annual variations over the lake area (see, e.g., Fig. 2). The lake's residuals show a decrease in the periods 1993-1995, 1996-1998, 2000-2002, 2005-2007, 2011-2013 and an increase in the period 2007-2011. While it might be assumed that the decreasing phase is the impact of relatively strong inter-annual variations of rainfall, the increasing phase in Lake Volta water level is attributed to the impact of a moderate La Niña event in 2007 triggering increased rainfall in the region (Paeth et al., 2012). It is worth mentioning, that besides the impacts of La Niña on the water level, the ponding of water behind the dam as mentioned in Section 4.5 could be a factor in the observed increase in water levels. Further, Owusu et al. (2008) attributed the lake level decline, which occurred between 2000 and 2002, and the relatively low maximum water levels

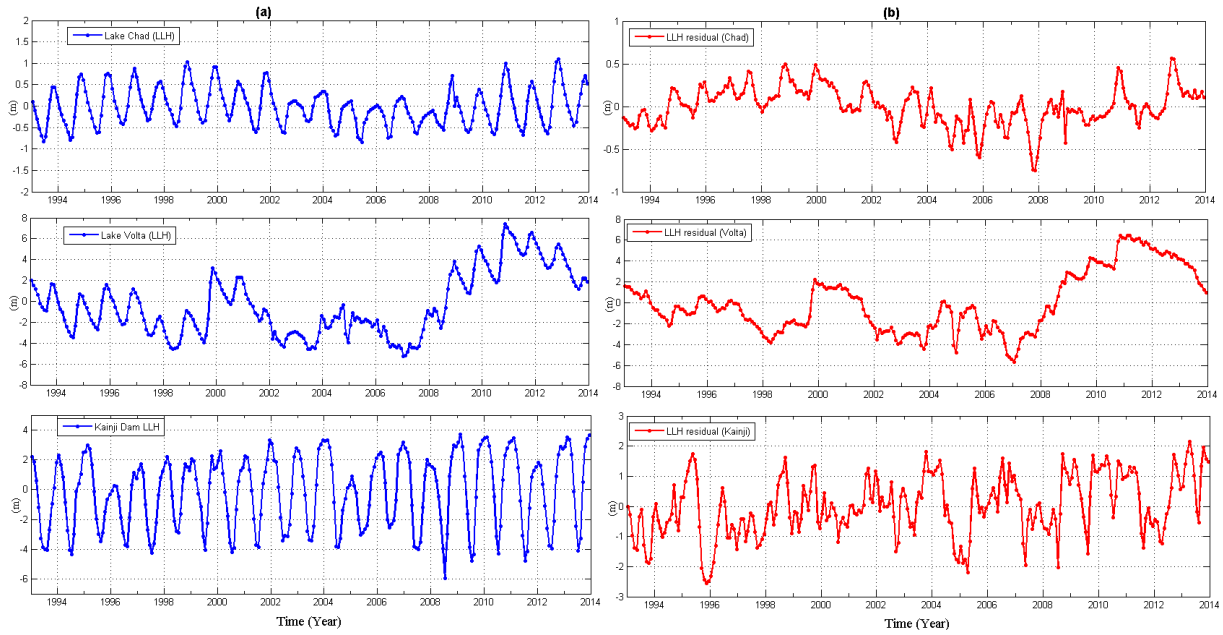

Figure 12: Analysis of lake water levels (a) Lake water levels before removing annual and semi-annual signals and (b) Lake water levels after removing annual and semi annual signals. * LLH-Lake Level Heights.

between 2002 to late 2007, to a decline in rainfall totals influenced by the warm phase of ENSO. Although the Lake Volta water levels between 2011 and 2014 show a gradual decline, however, the observed maximum water levels as captured in Fig. 12a and b still show a much higher maximum water level compared to the preceding decades, pointing towards water availability. Lake Volta, which has a total surface area of 8500 km^2 and stores approximately 150 km^3, is equipped with a hydropower generation capacity of more than 900 MW (Owusu et al., 2008). In view of the observed low minimum water levels (e.g., 1998, 2002-2004 and 2007 of Fig. 12a), the hydropower capacity of Lake Volta might be limited, and as reported in (Owusu et al., 2008) will lead to energy crises and conflicts amongst riparian countries who depend on this lake for energy production.

The Kainji dam is one of Nigeria's largest dam with a surface area of 130 hectares and primarily used for hydro-power generation (Ita et al., 1985). The dam supplies most of the domestic and industrial power needs of Nigeria and fluctuates seasonally according to the variability of rainfall. According to Jimoh (2008), semi-annual floods, which are separated by a period of 4 to 5 months and low water level between the months of March and May, occur at Kainji dam every year. The first part of this flood session, which originates from the head waters, arrives at Kainji in November and reaches its maximum in February while the second, which emanates from local tributaries, reaches Kainji in August and peaks in

September and October. This signal (i.e., semi-annual flood patterns) is part of the dominant multi-annual signals observed in our PCA results of GRACE-TWS (i.e., the second orthogonal mode), which is mostly visible over Guinea Coast and some parts of West Sahel (see Fig. 2). In addition, the observed maximum peaks reported in Jimoh (2008) due to inflow from local tributaries, which occurs in February and November, are also consistent with our altimetry observations for Kainji dam (Fig. 12a). Despite lacking a notable trend, relatively strong seasonal amplitudes, which correspond to intra-annual rainfall variability and water use, are observed in the residuals (see Fig. 12b).

While the lowest maximum water levels of Kainji reservoir observed in 1996 and 2005 (Fig. 12a) correspond to the lowest residuals shown in Fig. 12b of the same period, the lowest minimum observed water level (i.e., 2008) is not clearly marked out from the corresponding residuals indicated in Fig. 12b as they are dominated with more random signals that might be due to miss-fit to annual and semi-annual signals. However, since the maximum water levels of 2007 and 2011/2012 are not as strong for example, as those of 2002-2004, 2009-2010, and 2013 (Fig. 12a), the low minimum observed residuals of 2007 and 2011/2012 (Fig. 12b) might be the aftermath of those less pronounced maximum water levels (or relatively low maximum water levels) of 2007 and 2011/2012, while the low minimum residuals of 2008 (Fig. 12b) could be the result of the observed lowest minimum water level of 2008 in Fig. 12a. These observed minimum and low maximum water levels and the multi-annual fluctuations of the Kainji reservoir (Fig. 12a and b) are consistent with recent studies (Salami et al., 2011, 2015) that have reported a decrease in the reservoir inflow due to the development of infrastructures at the upstream of Kainji reservoir and changes in hydrological fluxes such as precipitation, evaporation, and temperature of the river Niger sub-basin where the dam is located.

Lakes, reservoirs, etc., respond naturally to climate and environmental conditions and can be used as indicators of water availability and water loss (Deus et al., 2013). Therefore, the observed low minimum water level residuals (i.e., 2005, 2007/2008, and 2011/2012) from our analyses and the decrease in the reservoir inflow at Kainji as reported by Salami et al. (2015) might be indicators to a water deficit in the Middle Belt region. In retrospect to our observed increase in water availability from the spatially averaged changes in TWS over West Africa (see Section 4.4), our analysis of the Kainji reservoir has indicated a water deficit triggered by low reservoir inflow. With decreased precipitation due to climate variability, reduced reservoir inflow, and the low residuals in water levels as observed in recent times, the hydrology of

the Kainji reservoir might undergo large changes that probably may impact negatively on the socio-economic prospects of the Middle Belt region.

5. Conclusions

In order to understand the changes in TWS over West Africa, this study used PCA and MLR to identify and analyse the dominant spatio-temporal variability of TWS and precipitation. Results from our analyses show that:

(i) High annual variability of GRACE-derived surface mass variations are observed in Guinea, Seirra Leone, Guinea Bissau, Liberia and Nigeria due to a considerable high rainfall amounts at seasonal and inter-annual time scales. The Lake Volta signal, which is largely dominated by multi-annual signals was identified from the PCA result.

(ii) Increasing multi-annual changes in TWS over riparian countries that constitute the Volta basin is also observed. This increase is seen as a response to intensified rainfall events due to ocean warming, and possibly the influence of ENSO in the region around the basin.

(iii) Precipitation over the region is dominated by annual and semi-annual signals influenced by circulation features, ocean warming, and climate tele-connections. Also, the region's susceptibility to drought conditions is also consistent with recent studies (e.g., Asefi-Najafabady and Saatchi, 2013; Panthou et al., 2012).

(iv) Analysis of TWS variability indicates a water deficit between 2002 and mid-2007 in the region. However, there is relative increase in water availability in recent times 2012-2014. Overall, the trend in TWS at Guinea between the period 2002 and 2014 is inconsistent with the linear trend in rainfall. This has been attributed to cumulative increase in the volume of water not involved in surface runoff, in addition to the water surplus from prolonged wet seasons, and lower evapotranspiration rates over the Guinea coast region.

(v) Despite the poor correlation of GLDAS TWSC in some parts of the region, the regression fit between the two variables (i.e., GRACE and GLDAS), with a coefficient of determination (R^2) of 0.85, however, indicates that trends and variability have been well modelled in most parts of the region. Further, the multi-linear regression (MLR) model simulates TWS and rainfall quite well using trend, annual, and semi-annual signals only, though some parts of the Central Sahel are poorly modelled. Considering the performance of the MLR model in TWS simulations for most parts of the region, changes in TWS can therefore be predicted quite well.

(vi) Increased magnitude in recent annual signals of Kainji reservoir as seen in the higher maximum and lower minimum water levels would imply increased flood/dry events throughout the year. These fluctuations coupled with relatively low maximum water levels of 2005, 2007/2008 and 2011/2012, which is also reflected in the observed residuals, might probably impact negatively on the socio-economic potentials of the Middle Belt region.

Lake Volta and the Kainji reservoir are largely used for hydroelectric power generation. With relatively strong annual and seasonal variability observed in these surface waters, their hydropower capacity might be limited in years where water levels are low. Despite the observed gradual decline in Lake Volta water level between 2011 and 2014, the observed maximum water level, which remains higher than in the preceding decades, points towards water availability in the Lake.

Appendix A

Generally as mentioned previously in Section 3.1.1, the CSR and JPL data sets are somewhat consistent for the region. However, there are some uncertainties in terms of the magnitudes estimated by the two products (Fig. 13 top). The time series of CSR data for the entire period before interpolation is also shown in Fig. 13 (bottom).

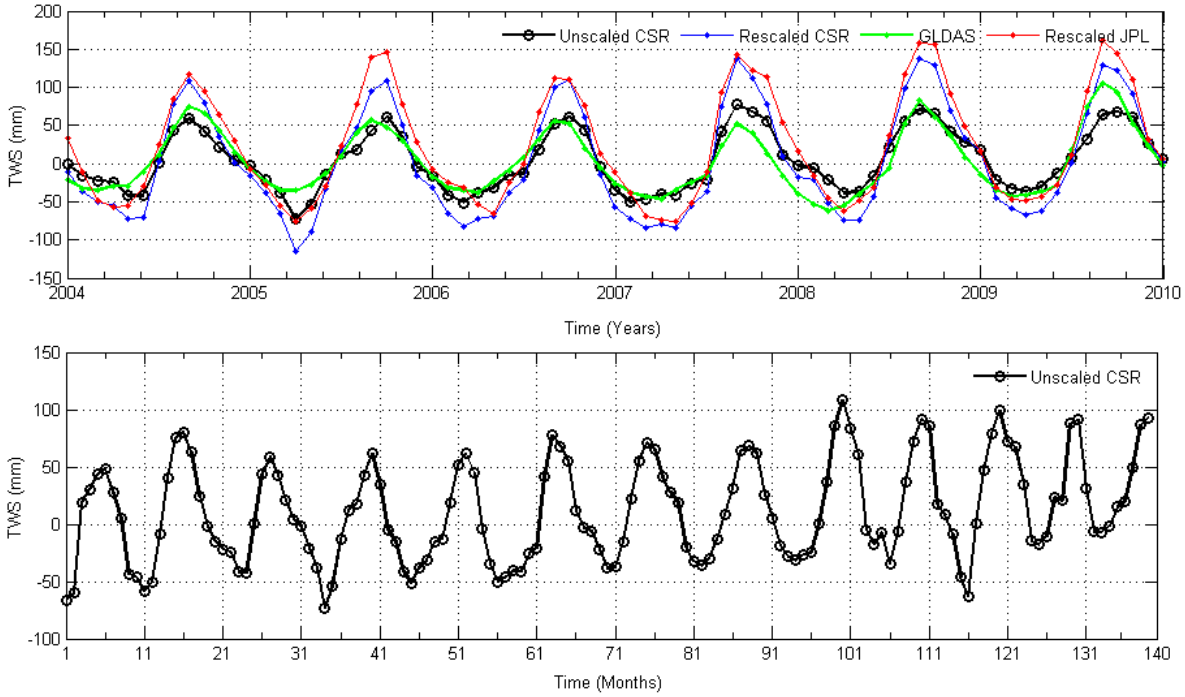

Figure 13: Time series of TWS from CSR, JPL, and GLDAS. The effect of the DDK2 filter on computed GRACE-derived TWS before and after restoring the geophysical signal loss is compared with the GLDAS-TWS (top panel). This comparison is done for the common time period were there are no data gaps in GRACE-derived TWS (i.e., 2003-2010). The bottom panel is the time series of GRACE-derived TWS (i.e., without restoring the signal loss caused by the DDK2 filter) before interpolation.

Acknowledgments

Christopher Ndehedehe is grateful to Curtin University for his PhD funding through the CSIRS programme, and University of Uyo, Nigeria, for the study leave. The Authors are grateful to CSR and NASA for the data used in this study. Joseph is grateful for the financial support of the Alexander von Humbodlt Foundation for supporting his stay at Institute of Technology (KIT, Germany) and Japan Society of Promotion of Science for supporting his stay at Kyoto University (Japan), the period during which part of this study was undertaken. He is grateful to the warm welcome and conducive working atmosphere provided by his hosts Prof. Bernhard Heck (Geodetic Institute, KIT, Germany) and Prof Yoichi Fukuda (Department of Geophysics, Kyoto University, Japan).

921 Adejuwon, J. (2006). Food security, climate variability and climate change in Sub Saharan
922 West Africa. *The International START Secretariat USA*. Assessments of Impacts and
923 Adaptations to Climate Change (AIACC).

924 Ahmed, M., Sultan, M., J.Wahr, and Yan, E. (2014). The use of GRACE data to monitor
925 natural and anthropogenic induced variations in water availability across Africa. *Earth*
926 *Science Reviews*, 136:289–300. doi:10.1016/j.earscirev.2014.05.009.

927 Amani, A., Thomas, J., and Abou, M. N. (2007). Climate change adaptation and water
928 resources management in West Africa. Synthesis report WRITESHOP. *UNESCO*. Retrieved
929 from: www.nlcap./net/032135.070920.NCAP. Accessed 15th April 2014.

930 Anayah, F. and Kaluarachchi, J. (2009). Groundwater resources of northern Ghana: Initial
931 assessment of data availability. *Unpublished Manuscript, Utah State University, USA*. Re-
932 trieved from: gw-a/frica.iwmi.org/Data/Sites/24/media/pdf/fieldreport-usu.pdf. Accessed
933 25 May, 2014.

934 Asefi-Najafabady, S. and Saatchi, S. (2013). Response of African humid tropical
935 forests to recent rainfall anomalies. *Transactions of the Royal Society*, 368:20120306.
936 doi:10.1098/rstb.2012.0306.

937 Awange, J., Forootan, E., Kuhn, M., Kusche, J., and Heck, B. (2014a). Water storage changes
938 and climate variability within the Nile Basin between 2002 and 2011. *Advances in Water*
939 *Resources*, 73(0):1 – 15. doi:10.1016/j.advwatres.2014.06.010.

940 Awange, J., Forootan, E., Kusche, J., Kiema, J., Omondi, P., Heck, B., Fleming, K., Ohanya,
941 S., and Gonalves, R. (2013). Understanding the decline of water storage across the Ramser-
942 Lake Naivasha using satellite-based methods. *Advances in Water Resources*, 60(0):7 – 23.
943 doi:10.1016/j.advwatres.2013.07.002.

944 Awange, J., Gebremichael, M., Forootan, E., Wakbulcho, G., Anyah, R., Ferreira, V., and
945 Alemayehu, T. (2014b). Characterization of Ethiopian mega hydrogeological regimes us-
946 ing GRACE, TRMM and GLDAS datasets. *Advances in Water Resources*, 74(0):64 – 78.
947 doi:10.1016/j.advwatres.2014.07.012.

948 Barbe, L. L., Lebel, T., and Tapsoba, D. (2002). Rainfall variability in West Africa

during the years 1950-90. *Journal of Climate*, 15(2):187–202. doi:10.1175/1520-0442(2002)015¡0187:Rviwad¿2.0.Co;2.

Boker, S. M., Xu, M., Rotondo, J. L., and King, K. (2002). Windowed cross correlation and peak picking for the analysis of variability in the association between behavioral time series. *Psychological Methods*, 7(3):338–555. doi:10.1037/1082-989X.7.3.338.

Boone, A., Decharme, B., Guichard, F., Rosnay, P. D., Balsamo, G., Belaars, A., Chopin, F., Orgeval, T., Polcher, J., Delire, C., Ducharne, A., Gascoin, S., Grippa, M., Jarlan, L., Kergoat, L., Mougin, E., Gusev, Y., Nasonova, O., Harris, P., Taylor, C., Norgaard, A., Sandholt, I., Ottle, C., Poccard-Leclercq, I., Saux-Picart, S., and Xue, Y. (2009). The AMMA Land Surface Model Intercomparison Project (ALMIP). *Bulletin of American Meteorological Society*, 90(12):1865–1880. doi:10.1175/2009BAMS27/86.1.

Cheng, M. K., Tapley, B. D., and Ries, J. C. (2013). Deceleration in the Earth's oblateness. *Journal of Geophysical Research*, 118:1–8. doi:10.1002/jgrb.50058.

Coe, M. T. and Foley, J. A. (2001). Human and natural impacts on the water resources of the Lake Chad basin. *Journal Of Geophysical Research*, 106(4):3349–3356. doi:0148-0227/01/2000JD900587509.00.

Common, P. (1994). Independent component analysis, A new concept? *Signal Processing*, 36:314–1994.

Descroix, L., Mahé, G., Lebel, T., Favreau, G., Galle, S., Gautier, E., Olivry, J. C., Albergel, J., Amogu, O., Cappelaere, B., Dessouassi, R., Diedhiou, A., Breton, E. L., Mamadou, I., and Sighomnou, D. (2009). Spatio-temporal variability of hydrological regimes around the boundaries between Sahelian and Sudanian areas of West Africa. *Journal of Hydrology*, 375(12):90–102. doi:10.1016/j.jhydrol.2008.12.012.

Deus, D., Gloaguen, R., and Krause, P. (2013). Water balance modelling in a semi arid environment with limited in situ data using remote sensing in lake Manyara, East African rift, Tanzania. *Remote Sensing*, 5:1651–1680. doi: 10.3390/rs5041651.

Diatta, S. and Fink, A. H. (2014). Statistical relationship between remote climate indices and West African monsoon variability. *International Journal of Climatology*, 34(12):3348–3367. doi:0.1002/joc.3912.

978 Druyan, L. M. and Fulakeza, M. (2015). The impact of the Atlantic cold tongue on West
979 African monsoon onset in regional model simulations for 1998-2002. *International Journal*
980 *of Climatology*, 35(2):275–287. doi:10.1002/joc.3980.

981 Duan, Z. and Bastiaanssen, W. G. M. (2013). First results from Version 7 TRMM 3B43
982 precipitation product in combination with a new downscaling calibration procedure. *Remote*
983 *Sensing of Environment*, 131(0):1–13. doi: 10.1016/j.rse.2012.12.002 131(0),1-13.

984 FAO (1983). Integrating crops and livestock in West Africa. *Food and Agriculture Organiza-*
985 *tion Of The United Nations*. Retrieved from:www.fao.org/docrep/004/x6543e/X6543E00.
986 Accessed 10 May, 2015.

987 FAO (1997). Irrigation potential in africa: a basin approach. *FAO Land and Water Bulletin*,
988 4. Retrieved from:https://books.google.com.au/books. Accessed 28 September, 2015.

989 Favreau, G., Cappelaere, B., Massuel, S., Leblanc, M., Boucher, M., Boulain, N., and Leduc, C.
990 (2009). Land clearing, climate variability, and water resources increase in semiarid southwest
991 Niger: a review. *Water Resources Research*, 45:W00A16. doi:10.1029/2007WR006785.

992 Ferreira, V., Andam-Akorful, S. A., He, X., and Xiao, R. (2014). Estimating water storage
993 changes and sink terms in Volta Basin from satellite missions. *Water Science and Engineer-*
994 *ing*, 7(1):5–16. doi:10.3882/j.issn.1674-2370.2014.01.0028.

995 Ferreira, V. G., Gong, Z., and Andam-Akorful, S. A. (2012). Monitoring mass changes in the
996 Volta River Basin Using GRACE satellite gravity and TRMM precipitation. *Boletim De*
997 *Ciencias Geodesicas*, 18(4):549–563. doi:/WOS:000313106300003.

998 Forootan, E., Kusche, J., Loth, I., Schuh, W. D., Eicker, A., Awange, J., Longuevergne, L.,
999 Diekkruger, B., and Shum, M. S. C. K. (2014). Multivariate prediction of total water storage
1000 changes over West Africa from multi-satellite data. *Surveys in Geophysics*, 35(4):913–940.
1001 doi:10.1007/s10712-014-9292-0.

1002 Frappart, F., Hiernaux, P., Guichard, F., Mougin, E., Kergoat, L., Arjounin, M., Lavenu, F.,
1003 Koit, M., Paturel, J.-E., and Lebel, T. (2009). Rainfall regime across the Sahel band in the
1004 Gourma region, Mali. *Journal of Hydrology*, 375(12):128– 142.

Gbuyiro, S. O., Ojo, O., Iso, M., Okoloye, C., and Idowu, O. (2001). Climate and water resources management. *WEDC conference Zambia*, 27:383–386. Retrieved from: www.wedc.lboro.ac.uk/resources/conference/27/Gbuyiro.pdf. Accessed 15 May 2015.

Giannini, A., Salack, S., Lodoun, T., Ali, A., Gaye, A., and Ndiaye, O. (2013). A unifying view of climate change in the Sahel linking intra-seasonal, interannual and longer time scales. *Environmental Research Letters*, 8:1–8. doi:10.1088/1748-9326/8/2/024010.

Gosset, M., Viarre, J., Quantin, G., and Alcoba, M. (2013). Evaluation of several rainfall products used for hydrological applications over West Africa using two high-resolution gauge networks. *Quarterly Journal of the Royal Meteorological Society*, 139:923–940. doi:10.1002/qj.2130.

Grippa, M., Kergoat, L., Frappart, F., Araud, Q., Boone, A., de Rosnay, P., Lemoine, J. M., Gascoin, S., Balsamo, G., Ottl, C., Decharme, B., Saux-Picart, S., and Ramillien, G. (2011). Land water storage variability over West Africa estimated by Gravity Recovery and Climate Experiment (GRACE) and land surface models. *Water Resources Research*, 47(5):W05549. doi:10.1029/2009wr008856.

Hassan, A. A. and Jin, S. (2014). Water Cycle and Climate Signals in Africa Observed by Satellite Gravimetry. *IOP Conference Series: Earth and Environmental Science*, 17:1–6. doi:10.1088/1755-1315/17/1/012149.

Heim, R. R. (2002). A review of twentieth-century drought indices used in the United States. *Bulletin of American Meteorological Society*, 83(8):1149–1165.

Henry, C., Allen, D. M., and Huang, J. (2011). Groundwater storage variability and annual recharge using well-hydrograph and GRACE satellite data. *Hydrogeology Journal*, 19:741–755. doi:10.1007/s10040-011-0724-3.

Hinderer, J., de Linage, C., Boya, J.-P., Gegout, P., Masson, F., Rogister, Y., Amalvict, M., Pfeffer, J., Littel, F., Luck, B., Bayerb, R., Champollion, C., Collard, P., Moigne, N. L., Diamentc, M., Deroussi, S., de Viron, O., Biancale, R., Lemoine, J.-M., Bonvalot, S., Gabalda, G., Bock, O., Genthon, P., Boucher, M., Favreau, G., Sguis, L., Delclaux, F., Cappelaere, B., Oi, M., Descloitresh, M., Galleh, S., Laurent, J.-P., Legchenko, A., and Bouink, M.-N.

(2009). The GHYRAF (Gravity and Hydrology in Africa) experiment: Description and first results. *Journal of Geodynamics*, 48:172–181. doi:10.1016/j.jog.2009.09.014.

Huffman, G. J., Adler, R. F., Bolvin, D. T., Gu, G., Nelkin, E. J., Bowman, K. P., Hong, Y., Stocker, E. F., and Wolff, D. B. (2007). The TRMM Multisatellite Precipitation Analysis (TMPA): Quasi-Global, Multiyear, Combined-Sensor Precipitation Estimates at Fine Scales. *Journal Of Hydrometeorology*, 8:38–55. doi:10.1175/JHM560.1.

Ita, E., Sado, E., Balogun, J. K., Pandogari, A., and Ibitoye, B. (1985). A preliminary checklist of inland water bodies in Nigeria with special reference to lakes and reservoirs. *Kainji Lake Research Institute*. Retrieved from: www.fao.org/docrep/005/t0360e/T0360E09.htm11. Accessed on 10th May, 2015.

James, G. K., Adegoke, J. O., Saba, E., Nwilo, P., and Akinyede, J. (2007). Sattelite-based assessment of the extent and changes in the mangrove ecosystem of the Niger Delta. *Marine Geodesy*, 30:249–267. doi: 10.1080/01490410701438224.

Jimoh, O. D. (2008). Optimised operation of Kainji reservoir. *AU J.T.*, 12(1):34–42.

Jolliffe, I. T. (2002). Principal component analysis (second edition). *Springer Series in Statistics*. Springer, New York.

Kummerow, C., Simpson, J., Thiele, O., Barnes, W., Chang, A. T. C., Stocker, E., Adler, R. F., Hou, A., Kakar, R., Wentz, F., Ashcroft, P., Kozu, T., Hong, Y., Okamoto, K., Iguchi, T., Kuroiwa, H., Im, E., Haddad, Z., Huffman, G., Ferrier, B., Olson, W. S., Zipser, E., Smith, E. A., Wilheit, T. T., North, G., Krishnamurti, T., and Nakamura, K. (2000). The Status of the Tropical Rainfall Measuring Mission (TRMM) after Two Years in Orbit. *Journal of Applied Meteorology*, 39(12):1965–1982. doi:10.1175/1520-0450(2001)040¡1965:TSOTTR¿2.0.CO;2.

Kusche, J. (2007). Approximate decorrelation and non-isotropic smoothing of time-variable GRACE-type gravity field models. *Journal of Geodesy*, 81(11):733–749. doi:10.1007/s00190-007-0143-3.

Kusche, J., Schmidt, R., Petrovic, S., and Rietbroek, R. (2009). Decorrelated GRACE time-variable gravity solutions by GFZ, and their validation using a hydrological model. *Journal of Geodesy*, 83(10):903–913. doi:10.1007/s00190-009-0308-3.

1062 Landerer, F. W. and Swenson, S. C. (2012). Accuracy of scaled GRACE terrestrial water
1063 storage estimates. *Water Resources Research*, 48(4):W04531. doi:10.1029/2011WR011453.

1064 Laux, P. (2009). Statistical modeling of precipitation for agricultural plan-
1065 ning in the Volta Basin of West Africa. *Doctoral dissertation, Mitteilun-*
1066 *gen/Institut fr Wasserbau, Universitt Stuttgart*, 179(198). Retrieved from:elib.uni-
1067 stuttgart.de/opus/volltexte/2009/4016/pdf/Dissertation-Laux.pdf. Accessed 25 July, 2014.

1068 Lebel, T. and Ali, A. (2009). A physical basis for the interannual variability of rain-
1069 fall in the Sahel. *Quarterly Journal Of The Royal Meteorological Society*, 375(1-2):5264.
1070 doi:10.1016/j.jhydrol.2008.11.030.

1071 Lebel, T., Cappelaere, B., Galle, S., Hanan, N., Kergoat, L., Levis, S., Vieux, B., Descroix,
1072 L., Gosset, M., Mougin, E., Peugeot, C., and Seguis, L. (2009). AMMA-CATCH studies in
1073 the Sahelian region of West-Africa: An overview . *Journal of Hydrology*, 375(12):3 – 13.

1074 Leblanc, M., Favreau, G., Tweed, S., Leduc, C., Razack, M., and Mofor, L. (2007). Re-
1075 mote sensing for groundwater modelling in large semiarid areas: Lake Chad Basin, Africa.
1076 *Hydrogeology Journal*, 15:97–100. doi: 10.1007/s10040-006-0126-0.

1077 L´Hôte, Y., Mahé, G., Somé, B., and Triboulet, J. P. (2002). Analysis of a Sahelian annual
1078 rainfall index from 1896 to 2000; the drought continues . *Hydrological Sciences Journal*,
1079 47(4):563–572. doi:10.1080/02626660209492960.

1080 Long, D., Longuevergne, L., and Scanlon, B. R. (2015). Global analysis of approaches for
1081 deriving total water storage changes from GRACE satellites. *Water Resources Research*,
1082 51(4):2574–2594. doi:10.1002/2014WR016853.

1083 Long, D., Scanlon, B. R., Longuevergne, L., Sun, A. Y., Fernando, D. N., and Save, H. (2013).
1084 GRACE satellite monitoring of large depletion in water storage in response to the 2011
1085 drought in Texas. *Geophysical Research Letters*, 40(13):3395–3401. doi:10.1002/Grl.50655.

1086 MacDonald, A. M., Bonsor, H. C., Dochartaigh, B. E. O., and Taylor, R. G. (2012). Quan-
1087 titative maps of groundwater resources in Africa. *Environmental Research Letters*, 7.
1088 doi:10.1088/1748-9326/7/2/024009.

1089 Marshall, M., Funk, C., and Michaelsen, J. (2012). Examining evapotranspiration trends in
1090 Africa. *Climate Dynamics,*, 38(9-10):1849–1865. doi:10.1007/s00382-012-1299-y.

1091 Martinez, W. L. and Martinez, A. R. (2005). *Exploratory Data Analysis with MATLAB.*
1092 Computer Science and Data Analysis Series. Chapman and Hall/CRC Press LLC, UK.

1093 McKee, T. B., Doeskin, N. J., and Kieist, J. (1993). The relationship of
1094 drought frequency and duration to time scales. *Conference on Applied Climatol-*
1095 *ogy, American Meteorological Society,Boston, Massachusetts*, pages 179–184. Retrieved
1096 from:www.ccc.atmos.colostate.edu/relationshipofdroughtfrequency.pdf. Accessed 27 June,
1097 2014.

1098 McKee, T. B., Doeskin, N. J., and Kieist, J. (1995). Drought monitoring with multiple
1099 time scales. *Conference on Applied Climatology, American Meteorological Society, Boston,*
1100 *Massachusetts*, pages 233–236. Retrieved from:www.southwestclimatechange.org/node/911.
1101 Accessed 13 July, 2014.

1102 McSweeney, C., New, M., Lizcano, G., and Lu, X. (2010). The UNDP climate change country
1103 profiles improving the accessibility of observed and projected climate information for studies
1104 of climate change in developing countries. *Bulletin of the American Meteorological Society*,
1105 91(2):157–166. doi:10.1175/2009BAMS2826.1.

1106 Moore, P. and Williams, S. D. P. (2014). Integration of altimetry lake lavels and GRACE
1107 gravimetry over Africa: Inferences for terrestrial water storage change 2003-2011. *Water*
1108 *Resources Research*, 50:9696–9720. doi:10.1002/2014WR015506.

1109 Nahmani, S., Bock, O., Bouin, M.-N., Santamara-Gmez, A., Boy, J.-P., Collilieux, X., Mtivier,
1110 L., Isabelle Panet, P. G., de Linage, C., and Wppelmann, G. (2012). Hydrological defor-
1111 mation induced by the West African Monsoon: Comparison of GPS, GRACE and loading
1112 models. *Journal of Geophysical Research-Solid Earth*, 117(B5). doi:10.1029/2011JB009102.

1113 Nguyen, H., Thorncroft, C. D., and Zhang, C. (2011). Guinean coastal rainfall of the West
1114 African Monsoon. *Quarterly Journal of the Royal Meteorological Society*, 137(660):1828–
1115 1840. doi:10.1002/qj.867.

1116 Nicholson, S. (2013). The West African Sahel: a review of recent studies on the
1117 rainfall regime and its interannual variability. *ISRN Meteorology*, 2013(453521):1–32.
1118 doi:10.1155/2013/453521.

1119 Nicholson, S. and Grist, J. (2001). A conceptual model for understanding rainfall variability
1120 in the West African Sahel on interannual and interdecadal timescales. *International Journal*
1121 *Of Climatology*, 21:1733–1757. doi:10.1002/joc.648.

1122 Nicholson, S. E. (2014). Spatial teleconnections in African rainfall: A comparison of 19th and
1123 20th century patterns. *Holocene*, 24(12):1840–1848. doi:10.1177/0959683614551230.

1124 Nicholson, S. E., Some, B., and Kone, B. (2000). An Analysis of Recent Rainfall
1125 Conditions in West Africa, Including the Rainy Seasons of the 1997 El Niño and
1126 the 1998 La Nia Years. *Journal of Climate*, 13(14):2628–2640. doi:10.1175/1520-
1127 0442(2000)013¡2628:AAORRC¿2.0.CO;2.

1128 Nicholson, S. E., Some, B., Mccollum, J., Nelkin, E., Klotter, D., Berte, Y., Diallo, B. M.,
1129 Gaye, I., Kpabeba, G., Ndiaye, O., Noukpozounkou, J. N., Tanu, M. M., Thiam, A., Toure,
1130 A. A., and Traore, A. K. (2003). Validation of TRMM and other rainfall estimates with a
1131 high-density gauge datasets for West Africa. Part I: Validation of GPCC rainfall product and
1132 pre-TRMM satellite and blended products. *Journal of Applied Meteorology*, 42:1337–1354.
1133 doi:10.1175/1520-0450(2003)042C1337:VOTAOR3E2.0.CO;2.

1134 Nicholson, S. E. and Webster, P. J. (2007). A physical basis for the interannual variability of
1135 rainfall in the Sahel. *Quarterly Journal Of The Royal Meteorological Society*, 133(629):2065–
1136 2084. doi:10.1002/qj.104.

1137 Odekunle, T. O. and Eludoyin, A. O. (2008). Sea surface temperature patterns in the Gulf
1138 of Guinea: their implications for the spatio-temporal variability of precipitation in West
1139 Africa. *International Journal Of Climatology*, 28:15071517. doi:10.1002/joc.1656.

1140 Ojo, O., Gbuyiro, S. O., and Okoloye, C. U. (2004). Implications of climate variability and
1141 climate change for water resources availability and management in West Africa. *GeoJournal*,
1142 61(2):111–119. doi:10.1007/s/10708-004-2863-8.

1143 Okonkwo, C., Demoz, B., and Gebremariam, S. (2014). Characteristics of lake Chad level
1144 variability and links to ENSO, precipitate, and river discharge. *The Scientifc World Journal*,
1145 13(4):13. doi:10.1155/2014/145893.

1146 Okpara, J., Tarhule, A. A., and Perumal, M. (2013). Study of climate change in niger river
1147 basin, west africa: reality not a myth. *INTECH Open science*. doi:10.5772/55186.

1148 Owusu, K., Waylen, P., and Qiu, Y. (2008). Changing rainfall inputs in the Volta basin:
1149 implications for water sharing in Ghana. *GeoJournal*, 71(4):201–210. doi:10.1007/s10708-
1150 008-9156-6.

1151 Oyebande, L. and Odunuga, S. (2010). Climate change impact on water resources at the
1152 transboundary level in West Africa: The cases of the Senegal, Niger and Volta Basins. *The*
1153 *Open Hydrology Journal*, 4:163–172. doi:10.2174/1874378101004010163.

1154 Paeth, H., Fink, A., Pohle, S., Keis, F., Machel, H., and Samimi, C. (2012). Meteorological
1155 characteristics and potential causes of the 2007 flood in sub-Saharan Africa. *International*
1156 *Journal of Climatology*, 31:1908–1926. doi:10.1002/Joc.2199.

1157 Panthou, G., Vischel, T., Lebel, T., Blanchet, J., Quantin, G., and Ali, A. (2012). Extreme
1158 rainfall in West Africa: A regional modeling. *Water Resources Research*, 48(8):W08501.
1159 doi:10.1029/2012wr012052.

1160 Pedinotti, V., Boone, A., Decharme, B., Crtaux, J. F., Mognard, N., Panthou, G., Papa, F.,
1161 and Tanimoun, B. A. (2012). Evaluation of the ISBA-TRIP continental hydrologic system
1162 over the Niger basin using in situ and satellite derived datasets. *Hydrology and Earth System*
1163 *Sciences*, 16(6):1745–1773. doi:10.5194/hess-16-1745-2012.

1164 Preisendorfer, R. (1988). Principal component analysis in meteorology and oceanography.
1165 *Developments in Atmospheric Science 17*. Elsevier, Amsterdam.

1166 Ramillien, G., Bouhours, S., Lombard, A., Cazenave, A., Flechtner, F. R., and Schmidt (2008).
1167 Land water storage contribution to sea level from GRACE geoid data over 2003-2006. *Global*
1168 *and Planetary Change*, 60(3-4):381–392. doi:10.1016/j.gloplacha.2007.04.002.

1169 Ramillien, G., Frappart, F., and Seoane, L. (2014). Application of the regional water mass
1170 variations from GRACE satellite gravimetry to large-scale water management in Africa.
1171 *Remote Sensing*, 6(8):7379–7405.

1172 Rangelova, E., van der Wal, W., Braun, A., Sideris, M. G., and Wu, P. (2007). Analysis of
1173 Gravity Recovery and Climate Experiment time-variable mass redistribution signals over
1174 North America by means of principal component analysis. *Journal of Geophysical Research:*
1175 *Earth Surface*, 112(F3):2156–2202. doi:10.1029/2006JF000615.

1176 Rieser, D., Kuhn, M., Pail, R., Anjasmara, I. M., and Awange, J. (2010). Relation between
1177 GRACE-derived surface mass variations and precipitation over Australia. *Australian Journal*
1178 *of Earth Sciences*, 57(7):887–900. doi:10.1080/08120099.2010.512645.

1179 Rodell, M., Houser, P. R., Jambor, U., Gottschalck, J., Mitchell, K., Meng, K., Arsenault,
1180 C. J., Cosgrove, B., Radakovich, J., Bosilovich, M., Entin, J. K., Walker, J. P., Lohmann,
1181 D., and Toll, D. (2004). The global land data assimilation system. *Bulletin of American*
1182 *Meteorological Society*, 85(3):381–394. doi:10.1175/BAMS-85-3-381.R.

1183 Roudier, P., Sultan, B., Quirion, P., and Berg, A. (2011). The impact of future climate change
1184 on West African crop yields: What does the recent literature say? *Global Environmental*
1185 *Change*, 21:1073–1083. doi:10.1016/j.gloenvcha.2011.04.007.

1186 Salami, A., Sule, B. F., and Okeola, O. (2011). Assessment of climate variability on Kainji
1187 hydropower reservoir. *Annual Conference of the National Association of Hydrological Sci-*
1188 *ences*. Hydrology for Sustainable Development and Management of Water Resources in the
1189 Tropic, Nigeria.

1190 Salami, A. W., Mohammed, A. A., Adeyemo, J. A., and Olanlokun, O. K. (2015). Assess-
1191 ment of impact of climate change on runoff in the Kainji lake basin using statistical meth-
1192 ods. *International Journal of Water Resources and Environmental Engineering*, 7(2):7–16.
1193 doi:10.5897/IJWREE2014.0513.

1194 Santos, J. a. F., Pulido-Calvo, I., and Portela, M. M. (2010). Spatial and tempo-
1195 ral variability of droughts in Portugal. *Water Resources Research*, 46(3):W03503.
1196 doi:10.1029/2009WR008071.

1197 Schuol, J. and Abbaspour, K. C. (2006). Calibration and uncertainty issues of a hydrological
1198 model (SWAT) applied to West Africa. *Advances in Geosciences*, 9:137–143. doi:adv-
1199 geosci.net/9/137/2006/.

1200 Seidou, O., Asselin, J. J., and Ouarda, T. B. M. J. (2007). Bayesian multivariate linear
1201 regression with application to change point models in hydrometeorological variables. *Water*
1202 *Resources. Research,*, 43:W08401. doi:10.1029/2001jb000576.

1203 Swenson, S., Chambers, D., and Wahr, J. (2008). Estimating geocenter variations from a

combination of GRACE and ocean model output. *Geophysical Research Letters*, 31:1–4. doi:10.1029/ 2004GL019920.

Swenson, S. and Wahr, J. (2002). Methods for inferring regional surface-mass anomalies from Gravity Recovery and Climate Experiment (GRACE) measurements of time-variable gravity. *Journal of Geophysical Research-Solid Earth*, 107(B9). doi:10.1029/2001jb000576.

Swenson, S. and Wahr, J. (2007). Multi-sensor analysis of water storage variations of the Caspian Sea. *Geophysical Research Letters*, 34(16). doi:10.1029/2007gl030733.

Tapley, B., Bettadpur, S., Watkins, M., and Reigber, C. (2004). The Gravity Recovery and Climate Experiment: Mission overview and early results. *Geophysical Research Letters*, 31:1–4. doi:10.1029/ 2004GL019920.

Thorncroft, C. D., Nguyen, H., Zhang, C., and Peyrill, P. (2011). Annual cycle of the West African monsoon: regional circulations and associated water vapour transport. *Quarterly Journal of the Royal Meteorological Society*, 137(654):129–147. doi:10.1002/qj.728.

USAID (2013). 2013 World population data sheet. *United States Agency International Development*. Retrieved from:www.prb.org. Accessed 2nd August 2014.

Verschoren, V. (2012). Trends in the hydrology of small watersheds in the Fouta Djallon Highlands. *Food and Agricultural Organization of the United Nations, Rome*. Retrieved from:http://www.fao.org/forestry/35845-051437ea2d60e968ba2e8ce3fbb3c3f95.pdf. Accessed 26 September, 2015.

Vierich, H. I. D. and Stoop, W. A. (1990). Changes in West African savanna agriculture in response to growing population and continuing low rainfall. *Ecosystems and Environment*, 31(2):115–132. doi: 10.1016/0167-8809(90)90214-X.

Wagner, S., Kunstmann, H., Brdossy, A., Conrad, C., and Colditz, R. (2009). Water balance estimation of a poorly gauged catchment in West Africa using dynamically downscaled meteorological fields and remote sensing information. *Physics and Chemistry of the Earth*, 34:25–235. doi:10.1016/j.pce.2008.04/.002.

Wahr, J., Molenaar, M., and Bryan, F. (1998). Time variability of the Earth's gravity field: Hydrological and oceanic effects and their possible detection using GRACE. *Journal of Geophysical Research-Solid Earth*, 103(B12):30205–30229. doi:10.1029/98jb02844.

1233 Wald, L. (1990). Monitoring the decrease of lake Chad from space. *Geocarto International*,
1234 5(3):31–36. doi: 10.1080/10106049009354266.

1235 Westra, S., Brown, C., Lall, U., Koch, I., and Sharma, A. (2010). Interpreting variability in
1236 global SST data using independent component analysis and principal component analysis.
1237 *International Journal of Climatology*, 30(3):333–346. doi:10.1002/joc.1888.

1238 WMO (2013). WMO statement on the status of the global climate in
1239 2012. *World Meteorological Organization*, WMO No.1108. Retrieved
1240 from:www.wmo.int/pages/prog/wcp/wcdmp/documents/WMO1108.pdf. Accessed 15th
1241 June, 2015.

1242 Wouters, B., Bonin, J. A., Chambers, D. P., Riva, R. E. M., Sasgen, I., and Wahr, J. (2014).
1243 GRACE, time-varying gravity, Earth system dynamics and climate change. *Reports on*
1244 *Progress in Physics*, 77(11):116801. doi:10.1088/0034-4885/77/11/116801.

1245 Xie, H., Longuevergne, L., Ringler, C., and Scanlon, B. R. (2012). Calibration and evaluation
1246 of a semi-distributed watershed model of Sub-Saharan Africa using GRACE data. *Hydrology*
1247 *and Earth System Sciences*, 16(9):3083–3099. doi:10.5194/hess-16-3083-2012.